INFORMATION BASED SENSOR CONTROL IN A TWO-VORTEX FLOWFIELD

BY

MAHMOUD MAMLOUK

THESIS

Submitted in partial fulfillment of the requirements
for the degree of Master of Science in Aerospace Engineering
in the Graduate College of the
University of Illinois at Urbana-Champaign, 2013

Urbana, Illinois

Adviser:

Professor Navaratnam Sri Namachchivaya

ABSTRACT

This thesis is divided in two parts. First, after presenting the modeling of the system in the deterministic and stochastic case, the controllability of one, then two Unmanned Aerial Vehicles (UAVs) manoeuvring in a two-vortex flow field is proven in the nonlinear case. In the second part, we develop a complete algorithm for optimally controlled sensor platform in a vortex flowfield. The question raised is: "How to control a UAV network evolving in a set of two vortices to collect the best data from these vortices?". The control part is based on information theory where the cost function is built using the the Kullback Leibler measure. The sensor platform is evolving in a vortex environment which is not controlled, yet has random initial conditions. Also, it is assumed that the UAVs are observed and that their positions are completely known. Thus we consider their dynamics as the only information available on the vortices. The sensor platform is in charge of finding the location that will contain the best information before actually getting the measurements from that place. We collect exclusively useful data by tracking the position that is expected to contain the best information using a specific information metric.

To my family and my future wife.

ACKNOWLEDGMENTS

First of all, I would like to thank from the bottom of my heart my adviser Dr. N. Sri Namachchivaya for granting me the opportunity to be part of his research group. The weekly individual and group meetings were a great opportunity to enhance my knowledge and learn new subjects. Professor Namachchivaya is not only a research adviser but also a life adviser, bringing his experience and wisdom to daily concerns. In addition, I would like to sincerely thank the Nonlinear System Group that warmly welcomed me in the laboratory and made me feel at home since the first day. I wish the best to all the members and a good luck in their prompt job search. They were also a great support in my research journey by answering all my questions and helping me solving my issues inside and outside the lab. I would also like to thank the Aerospace Engineering Department for giving me the opportunity to earn this Master degree and write this thesis. I would like to thank the Ecole Centrale de Lille and the BFI for trusting me to represent the school abroad through the double degree program that I am about to finish. I hope that I succeeded in my mission and that this is the beginning of multiple years of partnership. Finally, I would like to express all my love and gratitude to my family and my future wife who were always of a great support by encouraging all my initiative and my career choices. 2013 is my sixth year studying abroad, on two different continents, and I am always looking forward to go home and make them proud of my education accomplishments.

TABLE OF CONTENTS

LIST OF TABLES

LIST OF FIGURES

CHAPTER 1

INTRODUCTION

1.1 Motivation

Climate models, which require the study of high dimensional complex systems, are the best available tool for projecting likely climate changes. The past decade witnessed a chain of natural disasters related to climate change such as a larger number of high-intensity hurricanes, frequency and severity of tornadoes and severe thunderstorms, and increased wildfire activity across the United States, to name a few. These catastrophes are not only very hard to predict, but the damages that they cause are very serious and a lot of time and energy are spent to repair whatever can be repaired. According to the National Weather Service [1], weather event caused more than 1000 fatalities and 24 millions of dollars in total damages in 2011. More than half the fatalities are the result of tornadoes. They are massive flowfields that can destroy extended neighborhoods in minutes and a lot of work has to be done to minimize their consequences. We can for example try to develop a process that will accelerate evacuations by starting them at early points. This can only be done by a proper and accurate forecast of the evolution of the hurricanes and tornadoes in space and time. Forecasting of both their positions and intensity remain difficult even though they have improved over the last three decades.

Tornadoes dynamics are subject to a vortex-like representation that has been extensively studied throughout the past years. Paul K. Newton dedicated a whole book [9] to the derivation of these dynamics which turn out to be a weak solution to the Euler equations. A rigorous derivation can also be found in [8] where nonviscous flows are studied with a rigorous mathematical reasoning. The currently available model can have different hypothesis

[1] National Weather Service - http://www.nws.noaa.gov/om/hazstats/sum11.pdf

where the fluid is either ideal or viscous, rotational or irrotational and this can be reflected in the model equations in different way. We will present in this paper both the ideal and viscous fluid. In the case of viscous fluid, the viscosity introduces an extra uncertainty in the equations of motion. Relying on the models available, one can build a data assimilation scheme driven by the underlying uncertainties, that aims to extract as much information as possible from the flow-field to either predict its evolution in space or empirically improve the existing models.

Usually in data assimilation schemes, we are dealing with nonlinear stochastic systems that can be written as:

$$\begin{aligned} dX_t &= b(X_t, u_t)dt + \sigma_x(X_t)dW_t, \quad X_0 = x_0 \sim p(X_0) \\ dY_t &= h(X_t)dt + \sigma_y dV_t, \quad Y_0 = y_0 \sim \delta_{y_0} \end{aligned} \tag{1.1}$$

where X is the process associated with the system studied, in this case the position of the vortices with random initial condition and Y is the observation process. We assume that sensors are available and are sensing some quantities in discrete or continuous time. These processes are driven by independent white noise processes that dictate the statistics of the problem. Hence, a typical data assimilation problem contains model and parameter uncertainties, random initial conditions and sensor noise. Data assimilation blends the information from the observations with models to estimate the current state of a signal and to predict future states with certain probabillity. The data assimilation problem considered in this thesis requires a multifaceted approach that relies on a blend of multiple fields such as modeling, filtering, control and optimization. We will define some of these notions in the following.

1.2 Modeling

This section outlines fluid equations that are the basis for the vortex models presented in this thesis. We begin the formulation of the vortex dynamics by considering the Navier-Stokes (N-S) equations for describing the dynamics

of incompressible viscous fluid.

$$\frac{D\mathbf{u}}{Dt} = -\nabla p + \nu\nabla^2\mathbf{u} \quad \text{and} \quad \nabla\cdot\mathbf{u} = 0 \tag{1.2}$$

where $\frac{D}{Dt} = \frac{\partial}{\partial t} + \mathbf{u}\cdot\nabla$ is the material derivative and ν represents the viscosity coefficient. Alternatively, since $(\mathbf{u}\cdot\nabla)\mathbf{u}$ can be expressed as

$$(\mathbf{u}\cdot\nabla)\mathbf{u} = (\nabla\times\mathbf{u})\times\mathbf{u} + \frac{1}{2}\nabla(\mathbf{u}\cdot\mathbf{u})$$

the momentum equation of (1.2) can be rewritten as

$$\frac{\partial\mathbf{u}}{\partial t} + (\nabla\times\mathbf{u})\times\mathbf{u} + \frac{1}{2}\nabla(\mathbf{u}\cdot\mathbf{u}) = -\nabla p + \nu\nabla^2\mathbf{u} \quad \text{and} \quad \nabla\cdot\mathbf{u} = 0 \tag{1.3}$$

Defining the the vorticity vector $\omega \equiv \nabla\times\mathbf{u}$, observing

$$\nabla\cdot\omega = \nabla\cdot(\nabla\times\mathbf{u}) = 0 \quad (\text{since } \nabla\times\mathbf{u} \text{ orthogonal to } \nabla)$$

taking the *curl* of (1.2), and taking into account that the *curl* of a *gradient* vanishes, yields

$$\frac{\partial\omega}{\partial t} + (\mathbf{u}\cdot\nabla)\omega - (\omega\cdot\nabla)\mathbf{u} = \nu\nabla^2\omega \quad \text{and} \quad \nabla\cdot\mathbf{u} = 0 \quad \text{and} \quad \nabla\cdot\omega = 0 \tag{1.4}$$

Thus the vorticity formulation of the incompressible Navier-Stokes equation in 3 dimensions yields the vorticity equation

$$\frac{D\omega}{Dt} = (\omega\cdot\nabla)\,\mathbf{u} + \nu\nabla^2\omega \quad \text{and} \quad \nabla\cdot\omega = 0 \tag{1.5}$$

If $\nu = 0$, then one obtains the Euler's equations

$$\frac{D\omega}{Dt} = (\omega\cdot\nabla)\,\mathbf{u} \tag{1.6}$$

and it is obvious if $\omega = 0$ everywhere at any time t, then $\omega = 0$ always. Furthermore, ν can be thought of as diffusivity of the vortex and the diffusion of vorticity is analogous to the heat equation. Chorin's work [3] is based on viscous splitting under which the vorticity equations (1.5) are split into that corresponding to the Euler's equations (1.6) and the heat equation, that is,

in the tensor form,

$$\frac{D\omega_i}{Dt} = \omega_j \frac{\partial u_i}{\partial x_j} + \nu \frac{\partial^2 \omega_i}{\partial x_j \partial x_j} \tag{1.7}$$

For example, the second component reads

$$\frac{D\omega_2}{Dt} = \underbrace{\omega_1 \frac{\partial u_2}{\partial x_1}}_{\text{vortex turning}} + \underbrace{\omega_2 \frac{\partial u_2}{\partial x_2}}_{\text{vortex stretching}} + \underbrace{\omega_3 \frac{\partial u_2}{\partial x_3}}_{\text{vortex turning}} + \underbrace{\nu \left(\frac{\partial^2 \omega_2}{\partial x_1^2} + \frac{\partial^2 \omega_2}{\partial x_2^2} + \frac{\partial^2 \omega_2}{\partial x_3^2} \right)}_{\text{diffusion}} \tag{1.8}$$

By restricting to a two dimensional space, $\mathbf{u} = (u_1, u_2, 0)$ and $\frac{\partial}{\partial x_3} = 0$, then ω is parallel to the x_3 axis and $(\omega \cdot \nabla)\,\mathbf{u} = 0$ and (1.5) reduces to

$$\frac{D\omega}{Dt} = \nu \nabla^2 \omega \quad \text{and} \quad \nabla \cdot \omega = 0 \tag{1.9}$$

By definition $\omega \equiv \nabla \times \mathbf{u}$, and Biot-Savarat law inverts $\omega \equiv \nabla \times \mathbf{u}$ in the presence of the incompressibility condition, $\nabla \cdot \mathbf{u} = 0$, and allows one to construct the unknown velocity field $\mathbf{u}$ from the solution ω of the vorticity equation. Equation (1.8) is the starting point of the modeling of the vortex dynamics and the derivation of the point vortices from the Biot-Savarat law is discussed in detail in Chapter 2.

1.3 Filtering

Filtering Theory seeks to estimate the state of the system based on available observations by filtering out the noise that drives the process. Different algorithms are available in the literature, one has to choose the scheme that suits the need of the study as well as the characteristics of the system studied. For linear systems, assuming gaussian randomness, the Kalman Filter [25] is the most widely used filter where the random variable filtered is assumed to be Gaussian and thus only its expected value and its variance are sufficient to characterize it. This filter was extended to cover nonlinear systems (Extended Kalman Filter) as well as non Gaussian random systems that can be approached by a Gaussian representation (Ensemble Kalman Filter). In certain cases, having an approximation other than a gaussian distribution for the statistics of the underlying random variable can be appreciated. In fact, algorithms like Particle Filters [26] are meant to handle these kinds of

assumptions.

Kalman filters are useful because of their simplicity to implement and their low computational cost as well as robustness to high dimensions. On the other hand, particle filters can be used in the case of highly nonlinear systems where the distributions are approximated by as set of weighted particles.

1.4 Discrete Time Filtering Equations

In a general filtering problem, the quantity that we want to determine is the conditional law (conditional distribution) from which we estimate all the statistics that is needed. Probabilistic theory provides a recursive or a sequential filtering technique that estimates the system states sequentially by propagating information from the observation forward in time. In the discrete time case, filtering is divided into two distinct parts. The first step is usually called by two names the "propagation step" or the "forecast step" and the associated conditional distribution as a result of this step is called the "prior" distribution and the second step is called the"update", or the "analysis" and the updated conditional distribution is called the"posterior" distribution. We denote by a superscript p, the propagation (forecast) or the "prior" distribution π_k^p at time t_k, which is the conditional distribution of X_k given observations $Y_{0:k-1}$ up to time t_{k-1} and by a superscript u the posterior (filter) distribution or the updated conditional distribution π_k^u at time t_k, which is the conditional distribution of X_k given observations $Y_{0:k-1}$ up to time t_k. In principle, either by Kalman filter in the linear case or by nonlinear filter, these distributions can be computed recursively, alternating between propagation and update steps.

propagation: The propagation step leads from the posterior π_{k-1}^u (at time t_{k-1}) to **prior** π_k^p (at time t_k), where π_k^p is the distribution of the Markov process given by the plant $f(X_{k-1}, \xi_k)$ where $X_{k-1} \sim \pi_{k-1}^u$ and ξ_k is independent of X_{k-1} and has the distribution given by the evolution of the system Markov process.

update: The update step leads from π_k^p to the **posterior** π_k^u at time t_k and is

primarily the Bayes formula:

$$\pi_k^u(dx_k) \propto l(x_k|y_k)\pi_k^p(dx_k),$$

where l is likelihood for the state X_k given the observation Y_k. Since in all cases we assume linear observations with Gaussian noise

$$Y_k = H_k X_k + V_k, \quad Y_0 = 0 \quad \text{with} \quad V_k \sim N(0, R_k),$$

and the sensor noise covariance matrix R_k is assumed invertible. Hence, the likelihood for the state X_k given the observation Y_k is

$$l(X_k|Y_k) = \phi(Y_k; H_k X_k, R_k),$$

where $\phi(y; \mu, \Sigma)$ denotes the (in general multivariate) normal density with mean μ and covariance Σ of y.

1.4.1 Discrete Time Linear Filtering Equations

Here, we assume that given the state at $k-1$ and the linear map $A_k \stackrel{\text{def}}{=} A_{k-1\to k}$ to move from $k-1$ to k and the model error W_k we define the state X_k at k by the corresponding discrete time linear system

$$\begin{aligned} X_k &= A_k X_{k-1} + W_k, \quad \text{with} \quad W_k \sim N(0, Q_k) \\ X_0 &\sim N(\bar{x}, P) \quad \text{with Gaussin initial condition} \\ Y_k &= H_k X_k + V_k, \quad Y_0 = 0 \quad \text{with} \quad V_k \sim N(0, R_k), \end{aligned} \tag{1.10}$$

where W_k, V_k and the random initial conditions are independent. The observation at k and up to k are given and can be denoted as $Y_{0:k} = (Y_0, Y_1, \cdots, Y_k)$ and the sensor noise covariance matrix R_k is assumed invertible.

Once again we need to estimate the hidden state X_k given the past observations $Y_{0:k}$, Kalman filter estimates X_k by its first two moments, that is, the determination of the mean (estimator) vector $\hat{X}_k$ and the covariance matrix P_k that are given by Kalman filter equations.

Let us denote the **prior** state at t_k as X_k^p and **posterior** state at t_k as X_k^u. Then the propagation step leads to the two **prior** moments that are given

by the dynamics equations:

$$\begin{aligned} X_k^p &= A_k X_{k-1}^u, \quad \text{mean propagation} \\ P_k^p &= A_k P_{k-1}^u A_k^* + Q_k, \quad \text{covariance propagation} \end{aligned} \tag{1.11}$$

where the Kalman gain is given by

$$K_k = P_k^p H_k^* \left(H_k P_k^p H_k^* + R_k\right)^{-1}. \tag{1.12}$$

Similarly, the **posterior** moments are given by

$$\begin{aligned} X_k^u &= \boxed{X_k^p + K_k \left(Y_k - H_k X_k^p\right)} \quad \text{mean update} \\ &= X_k^p + P_k^p H_k^* \left(H_k P_k^p H_k^* + R_k\right)^{-1} \left(Y_k - H_k X_k^p\right) \\ &= A_k X_{k-1}^u + P_k^p H_k^* \left(H_k P_k^p H_k^* + R_k\right)^{-1} \left(Y_k - H_k X_k^p\right) \\ P_k^u &= P_k^p - K_k H_k P_k^p = \boxed{\left(I - K_k H_k\right) P_k^p} \quad \text{covariance update} \\ &= P_k^p - P_k^p H_k^* \left(H_k P_k^p H_k^* + R_k\right)^{-1} H_k P_k^p. \end{aligned} \tag{1.13}$$

Since the system is linear the "posterior" will have Gaussian distribution, i.e., $X_k^u \sim N(\mu_k^u, P_k^u)$ with the updated mean vector μ_k^u and covariance matrix P_k^u (take the expectation of (1.13)). Below we determine these two moments.

The updated mean vector is

$$\boxed{\mu_k^u = \mu_k^p + K_k \left(Y_k - H_k \mu_k^p\right).}$$

In the linear systems which are large dimensional, even the Kalman filter presents a serious computational difficulties. If the dimension n of the hidden state X is large, then the covariance matrices P_k^p and P_{k-1}^u are very large $m \times m$ matrices and storage and computations of K_k are very time consuming.

In this thesis we will use both Extended Kalman Filters (EKF) and Particle Filters. In the following we will give a brief description of the underlying algorithms.

1.4.2 Extended Kalman Filter

EKF is a recursive filtering algorithm that works in two steps. We recall that since the randomness is assumed normally distributed and the system is

linearized about the current mean and the covariance, we only need the mean and the variance to characterize the statistics of the state random variable. The EKF can be done in two steps, a prediction step and an update step. *The reader shall assume that we are looking for an estimation at the time k.*

The prediction step is the propagation of the available mean and covariance at time step $k-1$. The update step is when the current observation is blended with the forecast values to give the estimate at current time. These steps can be written as:

- Predict
  - $\hat{x}_{k|k-1} = b(\hat{x}_{k-1|k-1}, u_{k-1})$
  - $P_{k|k-1} = F_{k-1} P_{k-1|k-1} F_{k-1}^T + Q_{k-1}$
- Update
  - Innovation: $\tilde{y}_k = y_k - h(\hat{x}_{k|k-1})$
  - Innovation covariance: $S_k = H_k P_{k|k-1} H_k^T + R_k$
  - Kalman Gain $K_k = P_{k|k-1} H_k^T S_k^{-1}$
  - Update state estimation: $\hat{x}_{k|k} = \hat{x}_{k|k-1} + K_k \tilde{y}_k$
  - Update state covariance $P_{k|k} = (I - K_k H_k) P_{k|k-1}$

where Q_k and R_k are the covariances of the noise in the state and observation equation respectively, $F_{k-1} = \left.\frac{\partial b}{\partial x}\right|_{\hat{x}_{k-1|k-1}, u_{k-1}}$ and $H_k = \left.\frac{\partial h}{\partial x}\right|_{\hat{x}_{k|k-1}}$.

1.4.3 Particle Filter

Particle filters are based on a numerical approximation using Monte Carlo methods that allows the filtering process without the need for an exact analytic expression for the evolution of the state probability density.

This procedure is presented for the discrete case and it can also be easily extended to the continuous time case. EKF is straightforward to implement even though computational complexities may arise while trying to get the inverse of the innovation covariance or the Jacobian of the nonlinear state and observation dynamics.

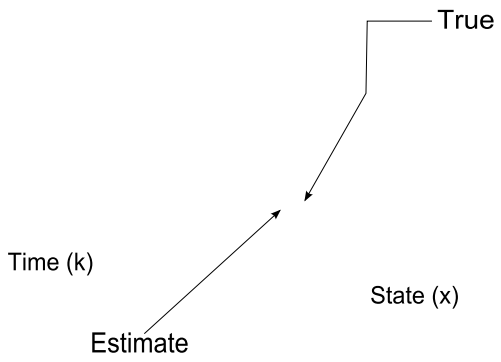

Figure 1.1: Particle Filtering Procedure

Figure 1.1 represents the different steps involved in particle filtering. Three distinct time steps are shown. The steps involved during one time step are summarized as follows,

1. At t_{k-1}, sample the distribution $p(x_{k-1}|y_1, \ldots, y_{k-1})$, N_s times and associate each sample with a probability weighting w_{k-1}. This gives us a set $\{x^i_{k-1}, w^i_{k-1}\}^{N_s}_{i=1}$.

2. Evolve each sample through the nonlinear system dynamics (1.1).

3. Update the weights associated with each sample when a new observation,y_k, becomes available according to; $w^i_k = w^i_{k-1} \frac{p(y_k|x^i_k)p(x^i_k|x^i_{k-1})}{q(x^i_k|x^i_{k-1}, y_k)}$ where q is the initial proposal density.

4. The evolved samples and their updated weights forms the discrete posterior density $p(x_k|y_1, \ldots, y_k)$ that is required.

The particle filter captures the nonlinear nature of the system unlike the EKF which makes a linear approximation to the system at each time step.

Both filters will be used in the estimation process of point vortices where the observations are collected with active tracers.

1.5 Control

1.5.1 Networks of Aerial and Oceanic Sensors

There is a need for near real-time integration of data from heterogeneous and spatially distributed oceanic sensors. A vast array of sensor platforms exists that include mooring systems, drifters with tracking devices, ships, aircraft, sea-gliders, and propeller-driven Autonomous Underwater Vehicles (AUVs). Drifters are typically deployed into the sea from a ship and on occasion from an airplane. Once floating within the ocean's surface water, a transmitter on the drifter sends a signal to Earth orbiting satellites which then relay the drifter's position to a receiving station. The data are then sent to the data assembly center where they are processed and distributed. Drifters may also house sensors which measure other ocean properties such as surface temperature, wind, ocean color, pressure, or salinity, and these data can also be transmitted through the satellite link.

Active sensors in the form of AUVs can be used for real-time ocean data collection for short term predictions and complement passive ocean sensors by traversing specific paths or accessing locations inaccessible to passive sensors. Gliders are buoyancy-driven vehicles that are slow but can remain deployed for several months at a time. Ships collect accurate data throughout the water column for chemical analyses. Aircraft can obtain snapshots of the sea-surface conditions in intervals of 5 hour or less, but with less accuracy than ships. The entire network of active and passive atmospheric and oceanic sensors (gliders, profiling floats, AUVs, remote sensing, ship-board observations, coastal radars and buoys) are linked in a large-scale control feedback loop for optimal sensor distribution and observing process for a global weather prediction and climate monitoring network.

Applicable observational data are essential climate variables (ECV) such as SST, wind velocity, temperature, current and mass transport. Through the developments of data assimilation and processing tools and methods, ECV data may be incorporated in the model for the simulation of ocean-atmosphere dynamics and the obtained results can be linked to climate change phenomena. The model of interest allows the combined analysis of processes of different time scales, by incorporating relevant ECV data into a single approximate model that captures the dominant and long-term dy-

namics of the coupled ocean-atmospheric system.

ECV data are provided by active and passive oceanic and atmospheric observing systems. Active systems, in the context of this proposal, are sensors for which we wish to develop active feedback control (see Section 4), such as AUVs. The aim of the control law for these sensors is to predict optimal sensor paths such that the most information rich data is collected at minimum operational costs. Passive systems, such as moored networks, drifting buoys, global observing satellites, and sondes are not subject to path control.

1.5.2 Sensor Control and Management

In an information rich environment of large, complex, and interacting systems, the task of state estimation and parameter identification become significantly more complicated as standard, centrally based approaches, cannot be in general implemented due to computational complexity. The state estimation problem relies on two fundamental ingredients, namely 1) sensor fusion: how to combine the measurements from different sensors, and 2) estimation: how to use the measurements to obtain the best possible state estimates. Estimation fusion, or data fusion for estimation, is the problem of how to best utilize useful information contained in multiple sets of data for the purpose of estimating an unknown quantity, a parameter or process at some time t. Practical reasons enforce distributed estimation of (local) variables based on a limited number of measurements from other stations. Fusion of local estimates to provide a global and accurate view of the dynamics is a key step in such a design.

With the emergence of sensing concepts that capitalize upon the rapidly increasing availability of controllable degrees of freedom, ranging from sensor operating mode to physical control of the platforms carrying the sensors, there is a need for new control methods for information collection. In the multi-sensor environment, the data assimilation problems rely on three fundamental ingredients, namely 1) sensor fusion: how to combine the measurements from different sensors, 2) estimation: how to use the measurements to obtain the best possible state estimates, and 3) maximization of information: optimal feedback strategies for information collection. The motion planning problem proposed in this thesis, considers the continuously extracted information along the motion of the mobile sensors and determines the steering

commands of the sensor platforms (UAVs, gliders, AUVs, remote sensing, ship-board observations, coastal radars and buoys).

In this thesis, we develop an optimal path planning formulation that maximizes the information gain by performing a sensor management scheme in the update step of the nonlinear filtering algorithm for a multi-sensor system. Our focus is on controlling the vehicles such that they maneuver to make observations that reduce the uncertainty (entropy of certain random variables of interest) efficiently. The dynamical system is the proposed climate model in the form

$$dX_t^\epsilon = b(X_t^\epsilon)dt + \sigma(X_t^\epsilon)dW_t, \tag{1.14}$$

which is observed by a collection of sensors,

$$dZ_t^\epsilon = h(Z_t^\varepsilon, X_t^\varepsilon; v(t))dt + \sigma(X_t^\epsilon, Z_t^\epsilon)dV_t, \tag{1.15}$$

and the observation process is modified from (1.15) to include control inputs $h(Z_t^\varepsilon, X_t^\varepsilon; v(t))$, $v : [0,T] \times \mathbb{R}^n \to \mathcal{U}_t \subset \mathbb{R}^k$, where n and k are the dimensions of the climate variables and that of the sensor control, respectively, and $\mathcal{U}_t$ is the permitted set of control values at time t.

Given a collection of sensors that are available at time t and a set of admissible control-inputs, our objective would be to maximize the information that can be gained about the state of climate variables X_t, by suitable placement of observing sensors which can be achieved by proper choice of $v(t)$. To this end we need a utility function $\mathcal{V}(x, v)$ which represents the information gain. The extent to which the new distribution (posterior) "differs" from the original a priori probability is a measure of the usefulness of the newly acquired data.

Since the Zakai equation is the central tool for understanding data assimilation in nonlinear dynamical systems, it leads to a number of more fundamental information-theoretic questions in this area:

- Which subsets of variables are more predictable than others?
- How can this be quantified?
- How can one estimate a lack of information in the observation beyond a forecast distribution?

A key tool to explore these *information theoretic* issues will be the Kullback-Leibler divergence and its connection with the the Zakai equation. A measure of the difference between the two distributions is relative entropy or the Kullback-Leibler distance. But since the true state of climate X_t is not known, one should be content to use an average of the utility, specifically $J(v) = \mathbb{E}[\mathcal{V}(x, v)]$, where

$$\mathcal{V}(x, v) \stackrel{\text{def}}{=} D(p_t^\varepsilon || q_t^\varepsilon) = \int p_t^\varepsilon(x, v) \, log \left(\frac{p_t^\varepsilon(x, v)}{q_t^\varepsilon(x)} \right) dx$$

is the Kullback-Leibler measure, or relative entropy, between the posterior $p_t^\varepsilon(x, v)$ and prior $q_t^\varepsilon(x)$. The utility function would be averaged with respect to observations. Our aim would be

$$\max_{v \in \mathcal{V}} J(v), \tag{1.16}$$

and maximizing J would amount to minimizing the uncertainty of the climate variable X_t due to the knowledge Y or maximizing the information gain.

This thesis will develop filtering algorithms that will improve predictability through relative entropy. This will quantify the lack of information in the observations in addition to estimating the state of the random dynamical system. Hence, the use of mutual information allows an optimal sensor placement and motion coordination strategy for mobile sensor networks.

1.6 Outline of the thesis

The purpose of this thesis is to design a control algorithm tailored for sophisticated sensor management and data collection systems composed of a network of Unmanned Aerial Vehicles (UAV), Autonomous Underwater Vehicles (AUV), and a network of drifters and moored sensors. The aim of the control law for these sensors is to predict optimal sensor paths such that the most information rich data is collected at minimum operational costs. We aim to design a controllable intelligent sensor platform that can be autonomously steered to sense measurements beneficial to state forecast and parameter estimation. The novel control algorithm is based on an information theoretic cost function that aims to improve the state estimation, by dynamically steering the measurement processes which are specifically

adapted to the complexities of the underlying flow.

In the second chapter, we will rigorously derive the equations of motion of a deterministic point vortex model as well as the dynamics of a set of tracers evolving in the vortex flow. We also present the extension to the stochastic model that covers the viscous case. The derivation goes back to solving the Euler equations for an ideal flow. We show that the Green function will be very useful in the resolution. We also give explicit solutions for one and two vortices and plot the Hamiltonian level curves for two and three vortex flows. Then, to design any control law that satisfies a certain objective, we have to make sure that the system is controllable. This will be the subject of the third chapter where the controllabilty different number of tracers in the nonlinear deterministic and stochastic flow is presented. Unlike the linear case, the nonlinear case requires more care in the construction of the controllability matrix using the Lie derivatives. Finally the fourth chapter presents the novel control algorithm based on information theory. We show the relationship between the problem that we are trying to solve (collecting measurements from information rich data) and the Kullback Leibler distance between the prior and posterior density of the state variable. We show how to use the filtering algorithms presented earlier to construct an adequate cost function as well as how to express that cost function explicitly. The results show an improvement in the amount of information that we were able to sense on the process as well as a reduction in the estimation error.

CHAPTER 2

SYSTEM PRESENTATION AND SET UP

2.1 System description

In this section, we will define the system dynamical equations and derive the point vortex model that will be used throughout the thesis.

2.1.1 N Vortex Dynamics

Definition 2.1.1. ***(Vorticity)*** *Given a flow-field with velocity* $\boldsymbol{u}$*=(u,v,w)* $\in \mathbb{R}^3$*, the associated vorticity is*

$$\omega = \nabla \times u \tag{2.1}$$

From now on, we will assume the following properties for the flow:

- inviscid flow (ideal, no viscosity)
- incompressible flow ($\nabla \cdot u = 0$)
- density = 1

Using the previous statements, one can write: $\nabla \cdot \omega = \nabla \cdot (\nabla \times u)$.
We notice that the vorticity ω and the velocity u satisfy the same type of differential equation. In fact, from the incompressibility of the flow, $\nabla \cdot u = 0$ and given (2.1), $\nabla \cdot \omega = \nabla \cdot (\nabla \times u) = 0$ (since $\nabla \times u$ is orthogonal to ∇). Thus, we end up with:

$$\nabla \cdot \omega = 0$$

$$\nabla \cdot u = 0$$

Furthermore, let us assume that the flow is rotational, which means that

there exists a potential ψ such that $\nabla \cdot \psi = 0$ and

$$u = \nabla \times \psi \tag{2.2}$$

We can derive a Poisson equation satisfied by Ψ that will appear to be convenient to solve for the vorticity of the system

$$\left.\begin{aligned} u &= \nabla \times \psi \\ \nabla \cdot \psi &= 0 \\ \omega &= \nabla \times u \end{aligned}\right\} \nabla^2 \psi = -\omega \tag{2.3}$$

Using (2.3), we can solve for ψ to get the flowfield vorticity ω. Then from (2.1), we can recover the velocity u. The process is straightforward as can be seen in the following steps.

To solve a Poisson equation, we can refer to multiple methods. In our case, we would like to find the solution of a Poisson equation on an open domain with a non zero right hand side. The use of Green's function comes in handy. The Green function is defined as the solution of the Poisson equation:

$$\nabla^2 G(\mathrm{x}) = -\delta(\mathrm{x}) \tag{2.4}$$

The solution of this equation is given by [9],

$$G(\mathrm{x}) = \begin{cases} -\dfrac{1}{2\pi} \log||\mathrm{x}|| & (\text{in } \mathbb{R}^2) \\ \dfrac{1}{4\pi} \dfrac{1}{||\mathrm{x}||} & (\text{in } \mathbb{R}^3) \end{cases} \tag{2.5}$$

Comparing (2.3) to (2.4), we assume that we can write ψ as:

$$\psi(\mathrm{x}) = -\int G(\mathrm{x} - z)\omega(z)dz \tag{2.6}$$

In the following, we shall introduce a fundamental parameter that characterizes a vortex, which is its intensity.

Theorem 2.1.1. ***(Circulation of the vorticity)*** *The intensity (or strength) of a vortex is given by the circulation of the velocity of the vortex on the con-*

tour domain.

$$\Gamma = \int_A \omega \cdot n dS = \oint_C u \cdot dl$$

where A is an open surface bounded by the closed curve C.

Now if we are in presence of an ideal and an incompressible fluid and in presence of conservative forces, the Kelvin circulation theorem states that the circulation of the vorticity is constant in time.

Theorem 2.1.2. ***(Kelvin Circulation Theorem)*** *If the fluid is ideal, incompressible and in presence of conservative forces:*

$$\oint_{\mathbb{C}(t)} \Gamma dS = constant \Leftrightarrow \frac{d\Gamma}{dt} = 0$$

2.1.2 The Two Dimensional case

We choose to study the N-Vortex system in two dimensions by looking at the dynamics in the horizontal cross-section.
In the two dimensional space we have:

$$\omega = \nabla \times u = \begin{pmatrix} \frac{\partial}{\partial x} \\ \frac{\partial}{\partial y} \end{pmatrix} \times \begin{pmatrix} u_1 \\ u_2 \end{pmatrix} = \frac{\partial u_2}{\partial x} - \frac{\partial u_1}{\partial y} = u_{2,x} - u_{1,y}$$

Thus, ω is one dimensional as well.

On the other hand, we know that $\nabla^2 \psi = -\omega$. So ψ is one dimensional. We call ψ, the *Scalar Stream Function.*
Given the scalar stream function, we can write the velocity u in two dimensions using (2.2):

$$u = \nabla \times \psi = \nabla^{\perp} \psi = \begin{pmatrix} 0 & 1 \\ -1 & 0 \end{pmatrix} \begin{pmatrix} \frac{\partial}{\partial x} \\ \frac{\partial}{\partial y} \end{pmatrix} \psi = (\psi_y, -\psi_x)$$

We notice that ψ behaves like a Hamiltonian for the fluid velocity. If we

consider one fluid particle, the equations of motion become:

$$u = \dot{\mathrm{x}} = (\dot{x}, \dot{y}) = (H_y, -H_x) = (\psi_y, -\psi_x)$$

$$\psi \longleftrightarrow H \quad \text{Hamiltonian}$$

$$\begin{cases} \dot{\mathrm{x}} = & \frac{\partial \psi}{\partial y} = & \frac{\partial H}{\partial y}(x, y, t) \\ \dot{y} = & -\frac{\partial \psi}{\partial x} = & -\frac{\partial H}{\partial x}(x, y, t) \end{cases}$$

Given that the scalar stream function can be assimilated into the Hamiltonian of the system and if we assume that flow is time independent, the level curves of the scalar stream function are the streamlines that the fluid particles follow with a tangent velocity.
We can calculate the normal vector to a level curve, it is given by the gradient of the Hamiltonian:

$$n = \nabla\psi = \nabla H$$

$$u \cdot n = \begin{pmatrix} \psi_y \\ -\psi_x \end{pmatrix} \cdot \begin{pmatrix} \psi_x \\ \psi_y \end{pmatrix} = 0$$

We notice that the fluid velocity is perpendicular to the Hamiltonian level curves. The streamlines are like "walls" that the fluid particle cannot penetrate. Depending on the initial conditions, if the fluid particle is placed on the level H_0 then it will evolve only on that level curve in the absence of noise. However, if the fluid is time dependent it is like those walls are moving. Thus, even though the particle is following a streamline, the value of the Hamiltonian at that level is still constant yet not spatially static. Figure 2.3 is a plot of the Hamiltonian level curves for a flowfield created by two vortices of equal strengths π.

2.1.3 Point Vortex Decomposition - Equations Of Motion of N Point Vortices

So far we have looked at the case where the vorticity has a support which is a hyperplan of the whole space $\mathbb{R}^3$. For N vortices, we have N of these supports in the plan. One can think about a special case where the vorticity is concentrated along a straight filament. In this case, we shrink the two dimensional supports to a set of singletons as shown in 2.1.

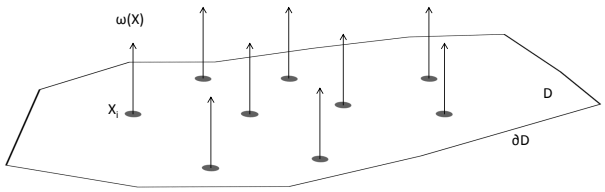

Figure 2.1: Vorticity Support

In general, for a discrete vortex representation in two dimensions, at any coordinate x at a constant altitude, the vorticity distribution is given by [9]:

$$\omega(\mathrm{x}) = \sum_{i=1}^{N} \frac{\Gamma_i}{2\pi} \phi_\epsilon(\mathrm{x} - \mathrm{x}_i) \tag{2.7}$$

$$\phi_\epsilon = \frac{1}{\epsilon^2}\, \phi(\frac{\mathrm{x}}{\epsilon}), \quad \epsilon \ll 1 \tag{2.8}$$

ϕ is assumed to be normalized ($\int \phi d\mathrm{x} = 1$) and radially symmetric. In the context of Point Vortex Representation, we take the limit as ϵ goes to zero in (2.7). The scalar stream function becomes:

$$\lim_{\epsilon \to 0} \phi_\epsilon(\mathrm{x}) = \delta(\mathrm{x})$$

and ω can be written as:

$$\omega(\mathrm{x}) = \sum_{i=1}^{N} \frac{\Gamma_i}{2\pi} \delta(\mathrm{x} - \mathrm{x}_i)$$

Remark: We insist on the fact that omega is discrete. In other words, there is a finite number of vortex filaments: $|\{\mathrm{x}, \omega(\mathrm{x})\}| = N$, finite.

From now on, we consider the flow irrotational.

As we see in (2.2), solving for u is equivalent to solving for ψ . Thus, lets use the point decomposition to solve for ψ invoking the Green function (2.4). Recalling (2.6), we only need G and ω to solve for ψ.

By definition, $\nabla^2 G(\mathrm{x}-z) = \delta(\mathrm{x}-z)$ in $\mathbb{R}^2$.

$$\begin{aligned}\nabla^2_{\mathrm{x}}\psi(\mathrm{x}) &= -\int_{\mathbb{R}^{\not 2}} \nabla^2_{\mathrm{x}} G(\mathrm{x}-z)\omega(z)dz \\ &= -\int_{\mathbb{R}^{\not 2}} \delta(\mathrm{x}-z)\omega(z)dz \\ &= -\omega(\mathrm{x})\end{aligned}$$

Since the stream function has a polar symmetry, $\psi(\mathrm{x}) = \psi(r)$. Then in polar coordinates:

$$\nabla^2 G(r) = \frac{d^2G}{dr^2} + \frac{1}{r}\frac{dG}{dr}$$

The Green function in polar coordinates is given by:

$$\begin{aligned}\nabla^2 G(r) &= \delta(r) \\ G'' + \frac{1}{r}G' &= 0 \quad \text{For } r > 0\end{aligned} \tag{2.9}$$

We can easily solve (2.9) since it is a homogeneous ordinary differential equation of the second order,

$$\begin{aligned}G(r) &= c_1 \log(r) + c_2 \\ &= c_1 \log(r), \quad \text{for} \quad c_2 = 0\end{aligned}$$

Theorem 2.1.3. ***(Green Theorem)*** *For all vector field F, we can relate the flux of F into a surface D to its circulation around the contour of F, ∂D:*

$$\iint_D \nabla \cdot F(\mathrm{x})d\mathrm{x} = \int_{\partial D} \boldsymbol{n} \cdot F(\mathrm{x})dl$$

where $\boldsymbol{n}$ is the normal vector to D at x.

Take $D = B(O, r)$ for all r and $F = \nabla G$, then

$$\begin{aligned}\iint_D \nabla \cdot \nabla G d\mathrm{x} &= \int_{\partial D} n \cdot \nabla G \, dl \\ \Leftrightarrow \iint_D \delta(\mathrm{x})d\mathrm{x} &= \int_{\partial D} n \cdot \nabla G \, dl\end{aligned} \tag{2.10}$$

Given $\iint \delta(\mathrm{x})d\mathrm{x} = 1$ and $\mathbf{n} = e_r$, we can write (2.10) as

$$\int_{\partial D} \frac{dG}{dr} dl = 2\pi r G'(r) = 1 \Leftrightarrow$$
$$G'(r) = \frac{1}{2\pi r} \Rightarrow c_1 = \frac{1}{2\pi}$$

Solving for G,

$$\begin{aligned} G(r) &= \frac{1}{2\pi}\log(r) \\ &= \frac{1}{2\pi}\log(\sqrt{x^2+y^2}) \\ &= \frac{1}{2\pi}\log(||\mathrm{x}||) \end{aligned}$$

which agrees with what was stated in (2.5).
Thus, $G(\mathrm{x}-\mathrm{z}) = \frac{1}{2\pi}\log(||\mathrm{x}-\mathrm{z}||)$. Suppose that a vortex i is located at $\mathrm{x}_i = (x_i, y_i)$, then

$$\begin{aligned} \dot{\mathrm{x}}_i &= u(\mathrm{x}_i, t) \\ &= \nabla^{\perp}\psi_i(\mathrm{x}, t) \end{aligned}$$

But, $\psi_i(\mathrm{x}, t) = -\int G(\mathrm{x}-\mathrm{z})\omega_i(\mathrm{z})d\mathrm{z}$. Thus, we can write the stream function for the vortex i as,

$$\psi_i(\mathrm{x}, t) = -\frac{\Gamma_i}{2\pi}\log(||\mathrm{x}-\mathrm{x}_i||)$$

We assume that all the vortices have equal contribution to the total flowfield. These contributions are weighed by the strength of each vortex. Hence if we look at the center of one vortex from the N vortex flow, its velocity is the same as one fluid particle placed in a flowfield created by $N-1$ distinct vortex centers. By the superposition principle one can write:

$$\begin{aligned}\dot{\mathrm{x}} = \sum_{i=1}^{N} \dot{\mathrm{x}}_i &= \sum_{i=1}^{N} \nabla^{\perp}\psi_i(\mathrm{x}, t) \\ &= \sum_{i=1}^{N} \frac{\Gamma_i}{2\pi}\left(\frac{\partial\psi_i}{\partial y}, -\frac{\partial\psi_i}{\partial x}\right) \\ &= \sum_{i=1}^{N} \frac{\Gamma_i}{2\pi}\left(\frac{y-y_i}{||\mathrm{x}-\mathrm{x}_i||^2}, \frac{x-x_i}{||\mathrm{x}-\mathrm{x}_i||^2}\right) \\ &= \sum_{i=1}^{N} \frac{\Gamma_i}{2\pi}\frac{(\mathrm{x}-\mathrm{x}_i)^{\perp}}{||\mathrm{x}-\mathrm{x}_i||^2} \end{aligned} \tag{2.11}$$

Each point vortex moves with the local velocity of the fluid and we can relate the velocity of the center of the vortex j to the positions of the center of the vortex i with $i \in [1, N] \setminus \{j\}$:

$$\dot{\mathrm{x}}_j = \sum_{i=1}^{N} \frac{\Gamma_i}{2\pi}\frac{(\mathrm{x}_j-\mathrm{x}_i)^{\perp}}{||\mathrm{x}_j-\mathrm{x}_i||^2} \tag{2.12}$$

We can also write the coordinates $\mathrm{x} = (x, y)$ in a the complexe form as $z_\alpha = x_\alpha + iy_\alpha$ where $i^2 = -1$.
The equations of motion (2.11) can be written as:

$$\dot{z}_j^* = -\frac{i}{2\pi}\sum_{i=1}^{N} \Gamma_j \frac{z_j - z_i}{|z_\alpha - z_i|^2} \tag{2.13}$$

where z^* is the complex conjugate of z.

2.1.4 Integrability of the Equations Of Motion

In the deterministic case that we have been looking at so far, we can verify whether or not these equations of motion are integrable and if the model chosen with the hypothesis can actually lead to an illustration of the vortices accurate enough to do the deterministic and stochastic controllability analysis. In [9], the integrability theorem is given up to $N = 4$.

Theorem 2.1.4. *The N vortex problem is integrable for $N \leq 3$ for any Γ_α, $\alpha \in \{1, 2, 3\}$.*

If $\Gamma = \sum_{\alpha=1}^{N} \Gamma_\alpha = 0$*, the 4-vortex problem is integrable.*

We will prove both cases $N = 1$ and $N = 2$.

Proof. Case $N = 1$: Consider a particle positioned at (x, y) in the flow field of an isolated point vortex of strength Γ located at the origin,

$$\dot{z}^* = -i\frac{\Gamma}{2\pi}\frac{z}{|z|^2} \Leftrightarrow \begin{cases} \dot{x} &= \frac{\Gamma}{2\pi}\frac{y}{\sqrt{x^2+y^2}} \\ \dot{y} &= \frac{\Gamma}{2\pi}\frac{x}{\sqrt{x^2+y^2}} \end{cases}$$

We apply the polar canonical transformation: $(x, y) \mapsto (\sqrt{2r}sin(\theta), \sqrt{2r}cos(\theta))$
After simple manipulations we get:

$$\begin{cases} \dot{r} &= 0 \\ \dot{\theta} &= \frac{\Gamma}{4\pi r} \end{cases}$$

The one vortex problem is easily integrable.
Case $N = 2$: Consider the motion of two vortices

$$\begin{cases} \dot{z}_1^* &= i\frac{\Gamma_2}{2\pi}\frac{z_1-z_2}{|z_1-z_2|^2} \\ \\ \dot{z}_2^* &= i\frac{\Gamma_1}{2\pi}\frac{z_2-z_1}{|z_1-z_2|^2} \end{cases}$$

Which can also be written as:

$$\begin{pmatrix} \dot{z}_1^* \\ \dot{z}_2^* \end{pmatrix} = \frac{i}{2\pi|z_1 - z_2|^2}\begin{pmatrix} \Gamma_2 & -\Gamma_2 \\ -\Gamma_1 & \Gamma_1 \end{pmatrix}\begin{pmatrix} z_1 \\ z_2 \end{pmatrix}$$

We can prove easily that $D^2 = |z_1(t) - z_2(t)|^2$ is a conserved quantity and hence equal to $|z_1(0) - z_2(0)|^2$. D is obviously the distance between the centers of the two vortices. This distance remains constant in time. The other conserved quantity is the position of the *center of vorticity* $C = \frac{\Gamma_1 z_1 + \Gamma_2 z_2}{\Gamma_1 + \Gamma_2}$.

Remarks:

- When $\Gamma_1 = \Gamma_2$, the vortices move on the same circle.
- When $\Gamma_1 + \Gamma_2 = 0$, the center of vorticity is at infinity and the vortices evolve on parallel lines with velocity $\sqrt{\frac{1}{2}(\Gamma_1^2 + \Gamma_2^2)}/2\pi D^2$

After simple manipulations, the equations can be decoupled to give:

$$\begin{pmatrix} z_1 \\ z_2 \end{pmatrix}^{*\prime} = i\frac{\Gamma_1+\Gamma_2}{2\pi D^2}\begin{pmatrix} 1 & 0 \\ 0 & 1 \end{pmatrix}\begin{pmatrix} z_1 - C \\ z_2 - C \end{pmatrix}$$

then using the same transformation as for the previous case, we can write:

$$z_1 - C = \sqrt{2R_1(t)}\exp(i\theta_1(t))$$
$$z_2 - C = \sqrt{2R_2(t)}\exp(i\theta_2(t))$$

which leads to:

$$\dot{R}_1 = 0 \qquad \theta_1 = \omega$$
$$\dot{R}_2 = 0 \qquad \theta_2 = \omega$$

where $\omega = \frac{\Gamma_1+\Gamma_2}{2\pi D^2}$. Thus, the ODE is easily integrable and the two vortex problem has a solution.

$N = 3$: we will leave the integrability of a particle placed in a 3-vortex environment as well as the interaction of three vortices for the next paragraph. □

2.1.5 Motion of Three Vortices

Consider three vortices of unit strength placed in an equilateral triangle configuration on the unit circle.
Since each side is of length $s = \sqrt{3}$, the triangle rotates rigidly with frequency $\omega = \sum_i 1/\Gamma_i 2\pi D^2 = 1/2\pi$. Since the vortices are placed on the unit circle, we can easily write their coordinates in the complex form as $z_j(t) = exp(i\theta_j(t))$. Assume $\theta_j(0) = 2\pi j/3$ which means $\theta_j(0) = 2\pi j/3 + t/2\pi$.
Then, the position of a particle placed in these three vortices is,

$$\dot{z}^* = i\frac{\Gamma_1}{2\pi}\frac{z - z_1}{|z - z_1|^2} + i\frac{\Gamma_2}{2\pi}\frac{z - z_2}{|z - z_2|^2} + i\frac{\Gamma_3}{2\pi}\frac{z - z_3}{|z - z_3|^2}$$

We perform the same coordinate transformation as in the previous paragraph: $z \mapsto \zeta exp(it/2\pi)$, then we can compute the Hamiltonian of the system

$$H = -\frac{1}{2}\sum_{j=1}^{3} \log|\zeta - exp(\frac{2\pi i}{3}j)|$$

Figure 2.2 below is a plot of the level curves of the Hamiltonian at $t > 0$. The level curves have the same shape as in the case where only two vortices were involved. We notice that around each vortex center there are some level curves that make the fluid particles always orbit around the center.

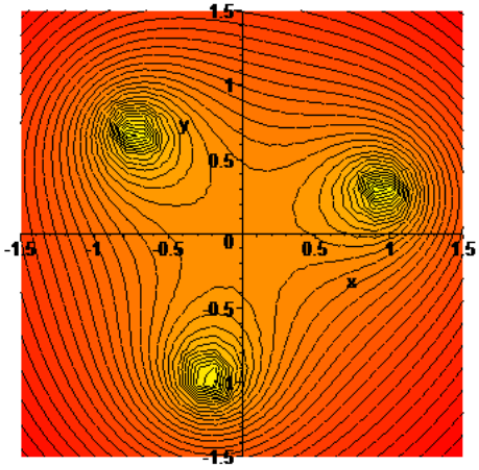

Figure 2.2: Hamiltonian Level Curves for a 3-vortex flow

2.1.6 Lagrangian Tracers

Lagrangian meters, such as ocean drifters and floats, provide a substantial part of ocean data which are used to reconstruct mean large-scale currents, estimate the rate of relative dispersion and give insight into the formation, movement and interactions of coherent structures such as point vortices. Lagrangian tracers, unlike Eulerian sensors, are evolving in the flow and their velocity will depend on the velocity of the flowfield at their position.

Trajectories of a Lagrangian tracer contain quantitative information about the dynamics of the of the underlying flow [4]; The fluid will steer the tracers as if it was part of the fluid but with a negligible mass. We can assimilate the tracer to a fluid particle evolving in the vortex flowfield.

Using (2.12), a tracer i is advected according to

$$\dot{\mathrm{y}}_t^i = \sum_j^N \frac{\Gamma_j}{2\pi} \frac{(\mathrm{y}_t^i - \mathrm{x}_t^j)^\perp}{|\mathrm{y}_t^i - \mathrm{x}_t^j|^2} \tag{2.14}$$

The coupling between the dynamical model of the vortices and the tracer allows us to extract maximal information about the vortices by tracking the tracer. We can also correct the model variables on the fly using data from the tracers. This data assimilation analysis will be treated in the last chapter of this paper.
We can track (under observability conditions) the velocity of the flow by placing these tracers in the fluid given a special care to their initial condition.

We can also write (2.24) in a complex form as:

$$\dot{z}^* = i \sum_j^N \frac{\Gamma_1}{2\pi} \frac{z - z_j}{|z - z_j|^2} \tag{2.15}$$

2.1.7 Examples

One very important special case is when the vortices have equal strength. For $\Gamma_1 = \Gamma_2$, the Hamiltonian can be written (under certain conditions) as:

$$H(x,y) = -\frac{1}{2}(x^2+y^2) + (1-\lambda)\log(\sqrt{(x+\lambda)^2+y^2} + \lambda\log(\sqrt{(x+\lambda-1)^2+y^2}$$

where $\Gamma_1 + \Gamma_2 = 2\pi$ and $\Gamma_2 = 2\pi\lambda$.
If $\Gamma_1 = \Gamma_2 = \pi$, the level curves are given in Figure 2.3
It is very important to denote that these plots depend on time and thus will be rotating clockwise or counter-clockwise depending on the signs of the intensities. They give an idea on the trajectory of a particle placed in the flow and evolving according to its dynamics.

The next section is an aside that will introduce a neat way to write the velocity of a particle in the space in the complex domain. It will be useful in the following sections.

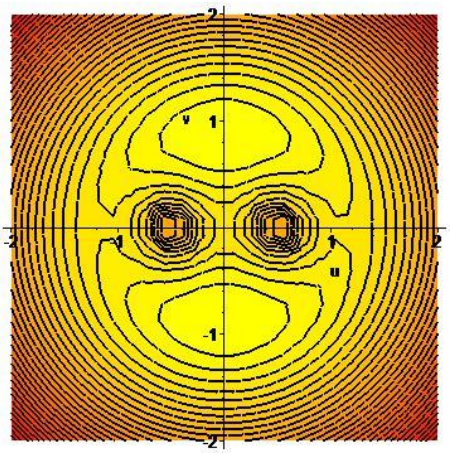

Figure 2.3: Hamiltonian Level Curves for $\Gamma_1 = \Gamma_2 = \pi$

2.2 Complex Notation

In this section, we will determine a complexe representation of the velocity of a particle in a time variant flowfield. In [11], we find a complex parameterization of the position and velocity of a point in the space when it is subject to a curvature (steering) control. We will develop this analysis in more details in the following paragraph.

In the Frenet-Serret frame, let us assume that e_T is a vector tangent to the curvature, e_N the normal vector and e_z to complete the basis with the right hand rule. Then we can write the Frenet-Serret equations of motion as:

$$\begin{aligned} \frac{de_T}{ds} &= \kappa e_N \\ \frac{de_N}{ds} &= -\kappa e_T + \tau e_z \\ \frac{de_z}{ds} &= -\tau e_N \end{aligned}$$

where s is the arclength, κ is the curvature and τ is the torsion.
If we assume that we are working with a normalized speed then the velocity vector is exactly e_T. We assume also that we have a planar motion which

makes all the components along e_z equal to zero. Thus, we end up with:

$$\begin{aligned} \dot{r} &= e_T \\ \dot{r} &= \kappa e_N \\ \frac{de_N}{ds} &= -\kappa e_T \end{aligned}$$

where $\dot{\mathrm{r}}$ is the unit velocity vector of the particle and hence the tangent vector to the particle trajectory. Using the same notation as in [11], we assume that a particle k is assimilated to a point material and we parametrize its position by r_k. Then, we build the Frenet frame of this particle.
The velocity is given by $\dot{\mathrm{r}}_k(t)$ and we can write in the Frenet frame,

$$\dot{\mathrm{r}}_k(t) = \mathrm{v} = v\mathrm{e}_t$$

where $v = ds/dt$ is the speed of the particle. Without loss of generality, we can assume that the particles are moving with a unit speed. Thus $v = 1$ and $\dot{\mathrm{r}}_k(t) = \mathrm{v} = \mathrm{e}_T$.
Let us denote θ_k the orientation of e_t with respect to the horizontal line. Then we have $\mathrm{e}_T = e^{i\theta_k}$. $\dot{\theta_k}$ is known as the *the curvature* of $\mathscr{C}$, the curve followed by the particle.
In conclusion, in a flow-free environment:

$$\begin{cases} \dot{\mathrm{r}}_k(t) = e^{i\theta_k} & \\ \dot{\theta_k} = u, & \text{curvature} \end{cases} \tag{2.16}$$

Below is a figure that summarizes the notations of this paragraph.

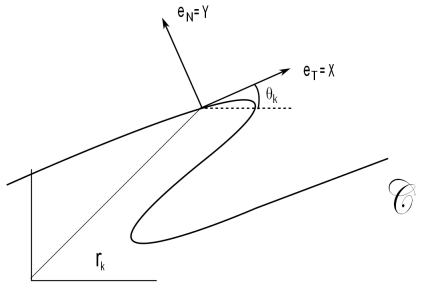

Figure 2.4: Complex Notation

2.3 The Two Vortex Stochastic Case

2.3.1 Vortex Equations of Motions for N=2

After examining the deterministic case where the major hypothesis was that the fluid is ideal, we can ask whether we can find an extension of this model that takes into account the viscosity of the flow. In fact, point vortex models that account for viscous effects also exist.
Chorin [3] introduced the first random point vortex method to simulate viscous incompressible flows. Later Marchioro and Pulvirenti in [7] considered a continuous-time random vortex method with Gaussian random walks replaced by independent Brownian motions and proved a corresponding mean field type result. It was shown by Marchioro and Pulvirenti [7] and Agullo and Verga [1] that a stochastic vortex dynamics model approximates the evolution of vorticity with viscosity, in the same way in which the deterministic vortex dynamics simulates the Euler equations. Vortex dynamics with viscosity are governed by set of Langevin or stochastic differential equations:

$$\dot{\mathrm{x}}_t^i = \sum_{j,j\neq i}^{n} \frac{\Gamma_j}{2\pi} \frac{\left(\mathrm{x}_t^j - \mathrm{x}_t^i\right)^{\perp}}{|\mathrm{x}_t^j - \mathrm{x}_t^i|^2} + \sqrt{2\nu}\xi_t^i \quad \text{with} \quad \mathrm{x}_0^i = \mathrm{x}^i, \tag{2.17}$$

where $\xi^i(t) \equiv (\xi_1^i(t), \xi_2^i(t))$ are zero mean white noise processes and equations (2.17) show that the velocity of each vortex is the sum of two terms, namely, the fluid velocity at the vortex position and a diffusive (stochastic) perturbation proportional to the fluid viscosity.

To understand the origin of the viscous term, we will show that the solution of (2.17) is the weak solution of the Navier-Stokes equation (1.5) [1]. Indeed, let us start with the vorticity for the point vortex model. We have,

$$\omega(x,t) = \sum_{i=1}^{N} a_i \delta(x - x_i(t)) \tag{2.18}$$

where $a_i = \Gamma_t/2\pi$. Taking the derivative of (2.18) and using (2.17),

$$\begin{aligned}
\frac{\partial}{\partial t}\omega(x,t) &= -\sum_{i=1}^{N} \frac{dx_i}{dt}(t) \cdot \nabla_{x_i}\delta(x - x_i(t)) \\
&= \sum_{i,j=1}^{N} a_i a_j \frac{a_j}{2\pi} \frac{\left(\mathrm{x}_t^j - \mathrm{x}_t^i\right)^{\perp}}{|\mathrm{x}_t^j - \mathrm{x}_t^i|^2} \cdot \nabla_x \delta(x - x_i) + \sqrt{2\nu} \sum_{i=1}^{N} a_i \xi_i \cdot \nabla_x \delta(x - x_i) \\
&= \sum_{j=1}^{N} a_j \sum_{i,j=1}^{N} a_i a_j \frac{a_j}{2\pi} \frac{\left(\mathrm{x}_t^j - \mathrm{x}_t^i\right)^{\perp}}{|\mathrm{x}_t^j - \mathrm{x}_t^i|^2} \cdot \sum_{i=1}^{N} a_i \nabla_x \delta(x - x_i) \\
&+ \sqrt{2\nu}\nabla_x \cdot \sum_{i=1}^{N} a_i \xi_i \delta(x - x_i) \\
&= -v(x,t) \cdot \nabla\omega(x,t) + \sqrt{2\nu}\nabla_x \cdot \sum_{i=1}^{N} a_i \xi_i \delta(x - x_i) \qquad (2.19)
\end{aligned}$$

This shows that the vorticity evolves according to a stochastic differential equation driven by the white noise process ξ.
The distribution of a white noise process is Gaussian with mean zero. Dimensional analysis shows that the variance of ξ - let us call it σ^2 - is proportional to the inverse of a time. We also recall that $dW = \xi dt$ and that $lim_{\Delta t \to 0} E[\Delta W(t)^2 - \Delta t] = 0$, where W is the Brownian Motion process which lead to $\sigma^2 = 1/(2dt)$ when $dt \to 0$.

We would like to take expectation (based on the white noise process ξ on both sides of (2.19)). Let us examine the last term of the right hand side,

$$\begin{aligned}
&E_{\xi_i}[\nabla_x \cdot \xi_i \delta(x - x_i)] \\
&= \int\int \frac{e^{-(\xi_{i1}^2 + \xi_{i2}^2)/2\sigma^2}}{2\pi\sigma^2} \left(\xi_{i1} \frac{\partial}{\partial x_1}\delta(x - x_i) + \xi_{i2} \frac{\partial}{\partial x_2}\delta(x - x_i) \right) d\xi_{i1} d\xi_{i2} \\
&= \sigma^2 E_{\xi_{i2}}[\int \frac{e^{-\xi_{i1}^2/2\sigma^2}}{\sqrt{2\pi\sigma^2}} \frac{\partial^2}{\partial\xi_{i1}\partial x_1}\delta(x - x_i) d\xi_{i1}] \\
&+ \sigma^2 E_{\xi_{i1}}[\int \frac{e^{-\xi_{i2}^2/2\sigma^2}}{\sqrt{2\pi\sigma^2}} \frac{\partial^2}{\partial\xi_{i2}\partial x_2}\delta(x - x_i) d\xi_{i1}] \\
&= \sigma^2 dt\sqrt{2\nu} \left(E_{\xi_1}[\frac{\partial^2}{\partial x_1^2}\delta(x - x_i)] + E_{\xi_2}[\frac{\partial^2}{\partial x_2^2}\delta(x - x_i)] \right) \\
&= \sqrt{\frac{\nu}{2}} E_{\xi_i}[\nabla_x^2 \delta(x - x_i)] \qquad (2.20)
\end{aligned}$$

where we used an integration by parts in the second equality as well as the identity

$$\frac{\partial}{\partial \xi_{j\alpha}}\delta(x-x_i) = \sqrt{2\nu}dt\delta_{ij}\frac{\partial}{\partial x_\alpha}\delta(x-x_i)$$

Now using these previous relations by substituting (2.20) in (2.19) we have,

$$E_{\xi_i}[\frac{\partial}{\partial t} + v(x,t)\,.\,\nabla\omega(x,t)] = \sqrt{2\nu}\sqrt{\frac{\nu}{2}}E_{\xi_i}[\sum_{i=1}^{N} a_i\nabla_x^2\delta(x-x_i)] \tag{2.21}$$

$$= E_{\xi_i}[\nabla_x^2\omega(x,t)] \tag{2.22}$$

which proves that (2.18) is indeed a weak solution of the Navier Stokes equation and that we can recover the velocity field from a vorticity under the form (2.18). We can also safely identify the parameter ν with the viscosity of the fluid.

We show that for two vortices, the state equation can be written in the following form:

$$\begin{pmatrix} \dot{x}_t^{11} \\ \dot{x}_t^{12} \\ \dot{x}_t^{21} \\ \dot{x}_t^{22} \end{pmatrix} = \frac{1}{2\pi r_t^2}\begin{pmatrix} -\Gamma_2 & 0 & \Gamma_2 & 0 \\ 0 & -\Gamma_2 & 0 & \Gamma_2 \\ \Gamma_1 & 0 & -\Gamma_1 & 0 \\ 0 & \Gamma_1 & 0 & -\Gamma_1 \end{pmatrix}\begin{pmatrix} x_t^{11} \\ x_t^{12} \\ x_t^{21} \\ x_t^{22} \end{pmatrix} + \sqrt{2\nu}\begin{pmatrix} \xi_t^{11} \\ \xi_t^{12} \\ \xi_t^{21} \\ \xi_t^{22} \end{pmatrix} \tag{2.23}$$

where $\mathrm{x} = (x^{11}, x^{12}, x^{21}, x^{22})^\top$ is the state vector containing the position of the vortex 1 and 2 respectively. Note that the flow is nonlinear because of the inverse of the distance squared.
We can also write (2.23) as

$$\dot{X}_t = A(X_t)X_t + \sqrt{2\nu}\xi_t \quad \text{with} \quad X_0 = X$$

where $A(X_t) = \frac{1}{2\pi r_t^2}\begin{pmatrix} 0 & -\Gamma_2 & 0 & \Gamma_2 \\ -\Gamma_2 & 0 & \Gamma_2 & 0 \\ 0 & \Gamma_1 & 0 & -\Gamma_1 \\ \Gamma_1 & 0 & -\Gamma_1 & 0 \end{pmatrix}$, $\xi_t = (\xi_t^{12}, \xi_t^{11}, \xi_t^{21}, \xi_t^{22})$ and $r_t^2 = (x_t^{21} - x_t^{11})^2 + (x_t^{22} - x_t^{12})^2$.

Now, we want to use a set of particles, namely Lagrangian tracers to collect the best amount of information from this flow. In [2], tracers have been used to collect such information. Their dynamics were given in terms of the flow

state. However, they were driven by the flow created by the vortices and they were completely passive. In chapter 4, we will introduce a control scheme to complete this work. As for now, let us examine the tracers' equations of motion in the following paragraph. This representation will form the foundations of the control design.

2.3.2 Tracer Equations Of Motion

Similarly to the vortices equations of motion, we can write the stochastic differential equations governing the dynamics of the particles while taking the viscosity into account:

$$\dot{\mathrm{y}}_t^i = \sum_j^n \frac{\Gamma_j}{2\pi} \frac{(\mathrm{y}_t^i - \mathrm{x}_t^j)^\perp}{|\mathrm{y}_t^i - \mathrm{x}_t^j|^2} + \sqrt{2\nu}\eta_t^i \quad \text{with} \quad \mathrm{y}_0^i = \mathrm{y}^i. \tag{2.24}$$

To be consistent with the notations that we used in the previous paragraph, we can write, by using Z_t^s as the particle 's' state, (2.24) as follows:

$$\dot{Z}_t^s = -\frac{1}{2\pi}\left(\frac{\Gamma_1}{(r_t^{s1})^2} + \frac{\Gamma_2}{(r_t^{s2})^2}\right) Z_t^s + \frac{1}{2\pi}\left(\frac{\Gamma_1}{(r_t^{s1})^2} + \frac{\Gamma_2}{(r_t^{s2})^2}\right) X_t + \sqrt{2\nu}\eta_t^s \tag{2.25}$$

where $(r_t^{sj}) = |Z_t^s - X_t^j|$, $j \in \{1, 2\}$ is the distance from the particle s to the vortex j. We shall transform (2.25) to the complex space to make use of the the Frenet frame:

$$\dot{Z}_t^s = \frac{J}{2\pi}\left[\Gamma_1 \frac{z_t^{s1} - x_t^{11}}{(r_t^{s1})^2} + \Gamma_2 \frac{z_t^{s1} - x_t^{21}}{(r_t^{s2})^2} + i\left(\Gamma_1 \frac{z_t^{s2} - x_t^{12}}{(r_t^{s1})^2} + \Gamma_2 \frac{z_t^{s2} - x_t^{22}}{(r_t^{s2})^2}\right)\right] + \sqrt{2\nu}\eta_t^s \tag{2.26}$$

$$= |\tilde{\dot{Z}}_t^s| e^{iarg(\tilde{\dot{Z}}_i^s)} + \sqrt{2\nu}\eta_t^s$$

$$= S_t^s e^{i\theta_t^s} + \sqrt{2\nu}\eta_t^s \tag{2.27}$$

where $\tilde{\dot{Z}}_t^s$ is the deterministic part of $\dot{Z}_t^s$.

CHAPTER 3

CONTROLLABILITY

The concept of controllability is extremely important in the context of linear and nonlinear systems, either deterministic or stochastic. Controllability theory gives a set of conditions that allow us to determine whether or not we can steer the system from its initial state to a target state. There are several categories of controllability, they include local controllability, global controllability, weak controllability, etc. In this section we will examine the controllability of a system formed by two vortices and a variable number of tracers. The purpose of this section is to come up with a set of conditions under which the system is controllable and make use of these conditions during the control design.

3.1 Nonlinear Deterministic Controllability Theory

The deterministic controllability is well defined for linear and non linear systems. We will only present the nonlinear case since the vortex-particle system is nonlinear. R. Hermann and A. Krener [12] studied the controllability of a nonlinear deterministic system

$$\Sigma : \begin{cases} \dot{x} &= f(x,u), \\ y &= g(x), \end{cases} \tag{3.1}$$

where the control variable u is in $\mathbb{R}^p$ subset of $\mathbb{R}^n$, $x \in \mathbb{R}^n$ and $y \in \mathbb{R}^m \subset \mathbb{R}^n$ is the observation variable.
If f and g are linear,

$$\dot{x} = Ax + Bu$$
$$y = Cx$$

then the controllability condition reduces to the well known rank condition, i.e,

$$\text{rank}(B|AB|A^2B|\cdots|A^{n-1}B) = n \tag{3.2}$$

To be more rigorous, let us define properly the different types of controllability.

Definition 3.1.1. ***(Controllability)*** *Define A as the set of points accessible from x_0. The system Σ is said to be controllable at x_0 if $A(x_0) = \mathbb{R}^n$.*
Furthermore, Σ is controllable, if $A(x_0) = \mathbb{R}^n$, for all $x_0 \in \mathbb{R}^n$.

This definition does not take into account if the travel time that is required for the state to reach any point in U. That is why we need *local controllability* as defined as follows,

Definition 3.1.2. ***(Local Controllability)*** *Σ is locally controllable at x_0 if for every neighborhood V of x_0, $A_V(x_0)$ is also a neighborhood of x_0.*
Σ is locally controllable if it is controllable at every point x of $\mathbb{R}^n$.

This definition describes the ability of the control to steer Σ from a state to the neighborhood of another.
Finally if we consider a neighborhood of the target state but also a neighborhood of x_0 then we define the **Weak controllability**.
In the case of nonlinear deterministic systems, the analysis found in [13] (based on [12] and [14]) is for systems of the form,

$$\dot{x} = f(x) + \sum_{i=1}^{p} g_i(x)u_i(x) \tag{3.3}$$

To state the controllability condition on systems of the form (3.3), we need one further definition.

Definition 3.1.3. ***(Lie Bracket)*** *Consider two vector fields f and g in $\mathbb{R}^n$. We define the Lie Bracket between f and g as,*

$$[f, g] = \frac{\partial g}{\partial x} f - \frac{\partial f}{\partial x} g$$

Also, higher order Lie Brackets can be defined,

$$\begin{aligned}(adj_f^1, g) &\triangleq [f, g] \\ (adj_f^2, g) &\triangleq [f, [f, g]] \\ &\cdots \\ (adj_f^k, g) &\triangleq [f, (adj_f^{k-1}, g)]\end{aligned}$$

where "ad" denotes the "adjoint".

The controllability condition for nonlinear deterministic systems can be stated using the Lie Brackets as defined above.

Theorem 3.1.1. ***(Controllability Rank Condition)*** *Equivalently to the version given for linear systems in* (3.2)*, we can define the rank condition that the system* (3.3) *has to satisfy in order to be controllable in the local sense about* x_0*, if the following matrix*

$$C = (g_1, g_2, \cdots, g_p, [g_i, g_j], \cdots, [ad_{g_i}^k, g_j], \cdots, [f, g_i], \cdots, [ad_f^k, g_i], \cdots) \quad (3.4)$$

has a full rank.

Comparing (3.4) to (3.2), we notice that the g_i terms are analogous to the B terms, the $[g_i, g_j]$ terms are representative of the nonlinearity of the system and finally the $[f, g_i]$ terms correspond to the AB term, etc.

Remark: If the system is driftless ($f(x) = 0, \forall x$), the full controllability is given by Chow's Theorem [15].
Now that the definitions are stated, let us verify the rank condition for the two-vortex system with one then two particles.

3.2 Application to the Two-Vortex System

To apply the theory stated above, we have to write the initial system (in the deterministic case) (2.11) and (2.24) in a form similar to (3.3). Let us consider two vortices and only one tracer. We denote the position vector of the vortices by $X = (X_1, X_2)^T = (x_1, x_2, x_3, x_4)^T$, where X_i is the vector

position of the vortex i. Similarly, for the tracer we denote its position by $Y = (y_1, y_2)^T$. With these notations, the equations of motion are,

$$\dot{X} = \begin{pmatrix} \dot{X}_1 \\ \dot{X}_2 \end{pmatrix} = b(X) = \begin{pmatrix} b1 \\ b2 \\ b3 \\ b4 \end{pmatrix}$$
$$\dot{Y} = a(X, Y) + g(u) = \begin{pmatrix} a_1 + u_1 \\ a_2 - u_2 \end{pmatrix}$$

where,

$$\begin{aligned}
b_1 &= \frac{\Gamma_2}{2\pi r^2}(x_4 - x_2) \\
b_2 &= \frac{\Gamma_2}{2\pi r^2}(x_1 - x_3) \\
b_3 &= \frac{\Gamma_1}{2\pi r^2}(x_2 - x_4) \\
b_4 &= \frac{\Gamma_1}{2\pi r^2}(x_3 - x_1) \\
a_1 &= \frac{\Gamma_1}{2\pi (r^1)^2}(x_1 - y_2) + \frac{\Gamma_2}{2\pi (r^1)^2}(x_4 - y_2) \\
a_2 &= \frac{\Gamma_1}{2\pi (r^1)^2}(y_1 - x_1) + \frac{\Gamma_2}{2\pi (r^1)^2}(y_1 - x_3).
\end{aligned}$$

It is noted that the control takes this particular form due to the fact that we plan to design it in order to modify the real and the imaginary parts of the tracer dynamics. The vortex dynamics are given by the nature and hence are not controllable. However, the control comes in the tracer dynamics which depend on the vortices dynamics. We shall then create an augmented system that will contain both vortex and tracer and verify the controllability condition on this latter. Let us denote $Z = (X, Y)^T$ the augmented vector.

The equations of motion become,

$$\dot{Z} = \begin{pmatrix} \dot{X} \\ \dot{Y} \end{pmatrix} = \begin{pmatrix} b1 \\ b2 \\ b3 \\ b4 \\ a_1 + u_1 \\ a_2 - u_2 \end{pmatrix} = f(Z, u) \tag{3.5}$$

To obtain a form similar to (3.3), one further transformation is needed. Let us denote $T = (Z, u)^T$ and $u + \dot{u} = v$. We can finally write the equations of motion for T as,

$$\dot{T} = \begin{pmatrix} \dot{Z} \\ \dot{u} \end{pmatrix} = \begin{pmatrix} f(Z, u) \\ v - u \end{pmatrix} \tag{3.6}$$

$$= \begin{pmatrix} f(Z, u) \\ -u \end{pmatrix} + \begin{pmatrix} 0 \\ v \end{pmatrix} \tag{3.7}$$

$$= l(T) + g_1 v_1 + g_2 v_2 \tag{3.8}$$

with $g_1 = (0, 0, 0, 0, 1, 0)^T$ and $g_2 = (0, 0, 0, 0, 0, 1)^T$.
Given the high dimension of the system as well as the high level of nonlinearities, we had to use a symbolic calculation software. We used Maple 15. We compute the rank condition by calculating the successive Lie Brackets and we find that rank(C) = 4 which is clearly different from the dimension of T (dim(T) = dim(Z) + dim(u) = 8). However this makes sense and actually proves that the system (3.6) is locally controllable. The rank that we found is exactly the dimension of the particle state plus the dimension of the control vector. To make sure that the controllable components are the ones corresponding to the particle and the control variable, we compute a basis of the space spanned by the matrix C. In fact, this basis is composed by the last four vectors of the canonical basis of $\mathbb{R}^8$.

In conclusion, we proved that **one tracer placed in a two vortex flowfield is locally controllable**.

We can now do the same analysis to two particles in a two vortex system. The vector T is now $T = (Z, u)^T = (x_1, x_2, x_3, x_4, y_1, y_2, y_3, y_4, v_1, v_2, v_3, v_4)^T$.

Again with the help of Maple, we find that the rank of the matrix C is 8 yet T has 12 dimensions this time. This also proves that two tracers in a two vortex flowfield are controllable since a basis of the subspace image of C is composed by the last eight vectors of the canonical basis of $\mathbb{R}^{12}$.
In conclusion, we proved that **two particles placed in a two vortex flowfield are locally controllable**.

In the next section we shall consider the stochastic equations of motion since the flowfield considered in this paper is a stochastic process.

3.3 Stochastic Controllability

Controllability of nonlinear systems was considered in the deterministic case for linear and nonlinear systems and the tools for proving any kind of controllability are discussed in several references. However, in the context of stochastic dynamics, global controllability was given less emphasis and several papers were devoted to its weak sense, which is to some extent, a stability analysis. Sunahara et al. [18] presented sufficient conditions for the controllability of nonlinear systems under several forms using a Lyapunov-like approach. Furthermore Zabczyk [17] derives necessary and sufficient conditions for global controllability of linear systems. An extension of this work is given in Ehrhardt and Kliemann [16]. They proved necessary and sufficient conditions for global controllability and showed that they reduce to the well known results for deterministic linear systems in the absence of noise. Recently, Mahmudov [20] showed the equivalence between proving the controllability for semi-linear and nonlinear systems and for the linearized version of the same systems. Besides these considerations, Sakthivel et al. [21] studied the complete controllability of nonlinear stochastic systems. The controllability condition presented in [21] relies on the condition that the associated linear system is completely controllable. Finally, Klamka [19] showed by generalized open mapping techniques sufficient conditions for constrained local stochastic controllability. In this thesis, two methods will be applied to prove the controllability of one tracer in a two vortex flowfield. These are presented in the following sections.

3.3.1 Nonlinear Stochastic Controllability Theory

This section will present a series of conditions that give necessary (and sometimes sufficient) conditions the prove the controllability of a stochastic nonlinear system of the form,

$$dX_t = f(X_t, u_t)dt + G(t, X_t)dW_t, \quad t \in [t_0, t_f] \tag{3.9}$$

where X_t is an n-dimensional stochastic process, u_t is an m-dimensional control vector and W_t a p-dimensional Brownian Motion process, f an n-dimensional real valued nonlinear function and G is the variance matrix with n rows and p columns.

Let us define the notion of controllability in the case of a stochastic system.

Definition 3.3.1. ***(ϵ Controllability [18])*** *An initial state x_0 is said to be stochastically ϵ-controllable in probability ρ, in the normal square sense, with respect to a specified target domain with the norm $\sqrt{\epsilon}$, in the time interval $[t_0, t_f]$, if there exists a control $u(t, X_t)$ such that*

$$P(||X_{t_f}||^2 \geq \epsilon | X_{t_0} = x_0) \leq 1 - \rho$$

where the norm $||.||$ is expressed as $\sqrt{X^T X}$.

Definition 3.3.2. ***(Complete ϵ-Controllability [18])*** *The system* (3.9) *is said to be completely ϵ-controllable in probability ρ in the normed square sense with respect to a specified target domain with the norm $\sqrt{\epsilon}$, in the time interval $[t_0, t_f]$, if and only if it is ϵ-controllable for every initial state x_0.*

Using these definitions, Sunahara et al. [18] proved the following theorem based on a Lyapunov type approach.

Theorem 3.3.1. ***(Stochastic ϵ-Controllability)*** *The initial state x_0 of the systems* (3.9) *is stochastically ϵ-controllable in probability ρ in the normed square sense with respect to the terminal state within $[t_0, t_f]$, if the following conditions are satisfied:*

Condition 1: For $t \in [t_0, t_f]$, there exists a scalar function $V(t, X)$ with bounded continuous first and second derivatives with respect to every compo-

nent of X and a first derivative with respect to $t \neq t_f$.

Condition 2: $V(t_f, X)$ satisfies

$$V(t_f, X) \geq \frac{1}{\alpha} X_{t_f}^T X_{t_f} \tag{3.10}$$

where $\alpha \geq 0$ such that $\alpha \ll \epsilon$.

Condition 3: A control $u(t, X)$ exists such that, along the trajectory obtained by solving (3.9) we have,

$$\mathcal{L}V \leq 0 \tag{3.11}$$

where $\mathcal{L}$ is the differential operator given by

$$\mathcal{L}(.) = \frac{\partial(.)}{\partial t} + f^T(t, X, u)\frac{\partial(.)}{\partial x} + \frac{1}{2} tr\left[G^T(t, X)\frac{\partial}{\partial x}\left(\frac{\partial(.)}{\partial x}\right) G(t, X)\right] \tag{3.12}$$

Condition 4: At the initial time t_0, V satisfies

$$V(t_0, x_0) \leq (1 - \rho)\frac{\epsilon}{\alpha} \tag{3.13}$$

The above theorem appears to be very restrictive and hard to implement. However, a closer look at the conditions will show that in our case, controllability and designing a control can be done and proven at the same time. Indeed, even though there are more conditions to be satisfied to be in the same context as the current study, they are relatively easy to fulfill. The next section, will apply the controllability as presented in [18] to the vortex and tracer problem.

3.3.2 Application to the two-vortex-1 tracer System

Consider the stochastic differential equation with multiplicative noise given by:

$$dX_t = F_t X_t dt + h_t(X_t)dt + C_t u_t(X_t)dt + X_t \sigma_t dW_t \tag{3.14}$$

where F and C are time dependent matrices of appropriate sizes. An approach similar to the one adopted in Theorem 3.3.1 can be used to prove the

controllability of the system (3.14). Indeed, it can be proven that if the four conditions presented above are augmented by two more conditions, we can obtain sufficient conditions on the controllability of (3.14).

Theorem 3.3.2. *The initial state of* (3.14) *is ϵ-stochastically controllable in probability ρ if Conditions 1 to 4 are satisfied in addition to conditions 5 and 6 below:*

Condition 5: There exists a bounded , symmetric and positive definite matrix S_t that satisfies the following Riccati equation:

$$\frac{dS}{dt} + S_t F_t + F_t^T S_t - S_t C_t C_t^T S_t + tr(\sigma_t^T \sigma_t) S_t = 0, \tag{3.15}$$

where S satisfies the terminal condition $S_{t_f} = \frac{1}{\alpha} I$

Condition 6: The nonlinear function h that appears in the SDE satisfies:

$$C_t q_t(X_t) + h_t(X_t) = -p(X_t) R_t X_t, \tag{3.16}$$

where q is a real-valued vector, p is a nonnegative real scalar and R is a matrix verifying $SR + R^T S$ is positive definite.

The proof can be found in [18].

Our system is clearly nonlinear and does not contain a multiplicative noise. A simple exponential transformation can lead to an equation in the form of (3.14). We can take the vortex problem as a nonlinear system that can be written as follows:

$$dX_t = b(X_t)dt + Cu(X_t)dt + \sigma dW_t \tag{3.17}$$

Let us consider the transformation $T = exp(X)$ and apply Ito formula to get

dT:

$$\begin{aligned} dT &= \frac{\partial exp(X_t)}{\partial t}dt + \frac{\partial exp(X_t)}{\partial X}\left(b(X_t)dt + Cu(X_t)dt + \sigma dW_t\right) + \frac{\sigma\sigma^T}{2}\frac{\partial^2 exp(X_t)}{\partial X^2}dt \\ &= \left(\frac{\partial exp(X_t)}{\partial X}b(X_t) + \frac{\sigma\sigma^T}{2}\frac{\partial^2 exp(X_t)}{\partial X^2} + Cu(X_t)\right)dt + \sigma\frac{\partial exp(X_t)}{\partial X}dW_t \\ &= \left(b(T_t)T_t + \frac{1}{2}\sigma\sigma^T T_t + Cu(T_t)\right)dt + \sigma T_t dW_t \\ &= b(T_t)T_t dt + \frac{1}{2}\sigma\sigma^T T_t dt + Cu(T_t)dt + \sigma T_t dW_t \end{aligned}$$

We can identify the terms in both equations as, $h_t(T_t) = b(T_t)T_t$, $F_t = \sigma\sigma^T/2$.

To relate these conditions to the vortex system observed with one tracer, we can solve the Riccati equation (3.15) explicitly to prove the existence of S. We will need to make use of the software Maple again which has a built-in function that solves classical matrix differential Riccati equations of the form:

$$\frac{dZ}{dt} = ZAZ + +ZK + K^T Z \tag{3.18}$$

This is far from being equivalent to the matrix differential equation of condition 5. However, when we take the vortex problem and the transformation previously done, condition 5 becomes:

$$\frac{dS}{dt} + S_t\frac{1}{2}\sigma\sigma^T + \frac{1}{2}\sigma^T\sigma S_t - S_t C_t C_t^T S_t + tr(\sigma_t^T\sigma_t)S_t = 0 \tag{3.19}$$

But σ can be written as: $\sigma = \sqrt{2\nu}$ and hence (3.19) becomes:

$$\frac{dS}{dt} + S_t\frac{1}{2}2\nu I + \frac{1}{2}2\nu I S_t - S_t C_t C_t^T S_t + 12\nu I S_t = 0 \tag{3.20}$$

We can now write(3.20) in a similar form to (3.18):

$$\frac{dS}{dt} + S_t\frac{1}{2}(2\nu + tr(\sigma_t^T\sigma_t))I + \frac{1}{2}(2\nu + tr(\sigma_t^T\sigma_t))I S_t - S_t C_t C_t^T S_t = 0 \tag{3.21}$$

Thus taking $A = CC^T$ and $K = -\frac{1}{2}(2\nu + tr(\sigma_t^T\sigma_t))I$, we can solve (3.21) with the terminal condition $S(t_f) = \frac{1}{\alpha}$ to get the matrix S:

$$\begin{pmatrix} \frac{e^{(-7\nu(t-t_f))^2}}{\alpha} & 0 & 0 & 0 & 0 & 0 \\ 0 & \frac{e^{(-7\nu(t-t_f))^2}}{\alpha} & 0 & 0 & 0 & 0 \\ 0 & 0 & \frac{e^{(-7\nu(t-t_f))^2}}{\alpha} & 0 & 0 & 0 \\ 0 & 0 & 0 & \frac{e^{(-7\nu(t-t_f))^2}}{\alpha} & 0 & 0 \\ 0 & 0 & 0 & 0 & \frac{14\nu e^{(-7\nu(t-t_f))^2}}{14\alpha\nu-1+e^{-14\nu(t-t_f)}} & 0 \\ 0 & 0 & 0 & 0 & 0 & \frac{14\nu e^{(-7\nu(t-t_f))^2}}{14\alpha\nu-1+e^{-14\nu(t-t_f)}} \end{pmatrix}$$

The proof of Theorem 3.3.2 requires a specific form of the Lyapunov function $V = X^T S X$. If we take $X = (x_1, x_2, x_3, x_4, y_1, y_2)^T$ where (x_1, x_2, x_3, x_4) are the coordinates of the two vortices and (y_1, y_2) are the coordinates of the tracer, V can be written as:

$$V = (x_1^2 + x_2^2 + x_3^2 + x_4^2)\frac{e^{(-7\nu(t-t_f))^2}}{\alpha} + (y_1^2 + y_2^2)\frac{14\nu e^{(-7\nu(t-t_f))^2}}{14\alpha\nu - 1 + e^{-14\nu(t-t_f)}}$$

Besides the form of V above (which can be easily shown to satisfy all the required conditions), the control is also given in specific form:

$$u_t(X) = -\frac{1}{2}C^T S_t X_t + q_t(X)$$

where S is the solution of the Riccati differential equation (3.21) and q satisfying Condition 6.
Now this form of control may appear to be restrictive, however it actually offers a certain freedom given that it has both a linear and a nonlinear part.

In conclusion, we proved the controllability of one and two tracers in a deterministic flow formed by two vortices. The proof was given using the classical methods of controllability matrix rank. Given the complexity of the flow, we chose to perform the calculations using Maple and we obtain the results that we expected. On the other hand, the stochastic case was more delicate. We can aim to find much simpler and less restrictive conditions to prove the controllability of a nonlinear stochastic system along the lines of the linear version presented in [19]. So far, only conditions on the linear part of the system are given to prove the controllability of the nonlinear system using the implicit function theorem.

CHAPTER 4

CONTROL DESIGN

After proving the controllability of the vortex system observed with one and two tracers, we can move forward by designing a control satisfying the objective that we aim to accomplish which is measuring useful information from the flow. We will define all the notions needed to state the cost function from an Information Theory point of view and will present an algorithm that will steer the tracers to information rich locations in the flow.

In this section we will introduce the discrete version of the system since it represents significant computational as well as algorithmic reasoning advantages. Then, we will show an improvement to the results proposed in the literature as far as vortex state filtering using one tracer and different filtering algorithms. Finally, we will introduce the control algorithm and show what are the areas of enhancement compared to the results without tracer control. As an illustrative example, control of a set of tracers to form a circular formation around a prescribed center is presented in the following section.

4.1 Complex Notation

If we place a particle s in a flowfield, its velocity will be given by the sum of its velocity with respect to the flow and the velocity of the flow with respect to the ground. Using (2.16),

$$\text{Velocity}_{particle/ground,flow-free} = \dot{\text{r}}_{1s}(t) = e^{i\theta_s} \tag{4.1}$$

$$\text{Velocity}_{particle/ground} = \text{Velocity}_{particle/flowfield} + \text{Velocity}_{flowfield/ground}$$

$$\text{Velocity}_{particle/flowfield} = \text{Velocity}_{particle/ground,flow-free} \tag{4.2}$$

where $\text{Velocity}_{particle/ground,flow-free}$ is the velocity of a particle with respect to the ground in a flow free environment and $\text{Velocity}_{particle/flowfield}$ is the velocity of a particle in a flowfield in the frame related to the flowfield and hence it can be seen (from the flowfield point of view) as a particle moving in a fixed frame.
We consider that the velocity is normalized (unit speed) and that the velocity vector is simply given by the tangent unit vecor to the curvature. Furthermore, θ_s is orientation of this vector with respect to the horizontal line, which is called "curvature".
Using (4.1) and (4.2), we get:

$$\begin{aligned} \dot{\mathrm{r}}_s(t) =& \dot{\mathrm{r}}_{1s}(t) + f_s(t) \\ =& e^{i\theta_s} + f_s(t) \end{aligned} \tag{4.3}$$

where $f_s(t) = f(r_s, t)$ is the velocity of the flow relative to the ground at the coordinate r_s. We can also write (4.3) as function of its modulus and argument as in (2.16):

$$\begin{aligned} \dot{\mathrm{r}}_s =& f_s(t) + e^{i\theta_s} \\ =& S_s e^{i\gamma_s} \end{aligned}$$

The steering of these particles with the control will be on $\dot{\gamma}_s = v$. In conclusion,

$$\begin{cases} \dot{\mathrm{r}}_s(t) = S_s e^{i\gamma_s} \\ \dot{\gamma}_s = v, \qquad\qquad \text{control} \end{cases} \tag{4.4}$$

4.1.1 Circular Formation around a Prescribed Center

One can think of steering the particles in a fluid flow vector field in such a way that the particles will perform a circular formation around a given target point in the two dimensional space. A geometric control [10] has been proven to steer the particles in a collaborative way to adopt a stable circular formation around a prescribed center. Paley [10] discussed several cases where the flowfield is either known or estimated and the target center

is arbitrary or prescribed. The control is given on the curvature as follows:

$$\dot{\gamma}_t^s = R[S_t^s + K(< e^{i\gamma_t^s}, P\mathbf{c} > + a_{s0} < e^{i\gamma_t^s}, c_t^s - \bar{c}_t >)] \tag{4.5}$$

- $R = \dot{\theta}_t^s$ is the curvature in a flow-free environment.
- $c_t^s = r_t^s + R^{-1} i \frac{\dot{r}_t^s}{|\dot{r}_t^s|}$ is the center of the circular trajectory of radius R of the particle 's' (this is the arbitrary center of any circular formation).
- $\bar{c}_t$ is the prescribed center
- P is the Laplace Matrix
- a_{s0} is the communication matrix where $a_{s0} = 1$ if the particle s is aware of the prescribed center 0 and $a_{s0} = 0$ otherwise.
- $< ., . >$ is a vector product in the Hilbert space such that $< \mathrm{x}, \mathrm{y} >= Re(\bar{\mathrm{x}}\mathrm{y})$
- K is a free adjustable parameter that depends on the turn rate. The portion in the control (4.5) that K multiplies $(a_{s0} < e^{i\gamma_t^s}, c_t^s - \bar{c}_t >)$ is what steers the particle to the prescribed circle center so it needs to be big enough that the portion of the control can pull it to where it needs to go

Simulations

We can apply the previous geometric control to the two vortex dynamics discussed in section 2.3. The following are two plots illustrating (4.5). The first shows three particles in a two vortex flow, performing a circular formation of radius $R = 1$ around the prescribed center $(1, 1)$. The second plot show three particles performing a circular formation around the center of one of the vortices which are moving targets.

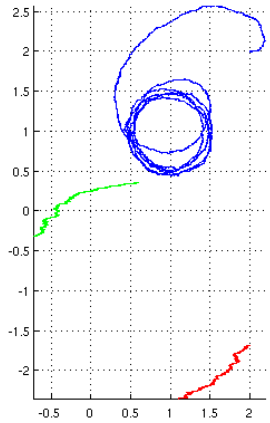

Figure 4.1: Circular formation around a prescribed center $(1, 1)$ with a radius $R = 1$

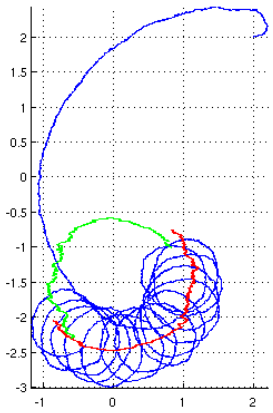

Figure 4.2: Circular formation around a vortex center

4.2 Two Vortex - One Tracer Filtering

In a climate problem with large scale circulations where the the states are changing very slowly, we expect to have observations very spread apart in time. The point vortex model presented in Section 2.1.3 can be used as an idealized model to study tornadoes and hurricanes. Furthermore, Global Positioning Systems (GPS) become more and more sophisticated as they provide almost continuous time data when observing the tracer position. We can then construct a discrete version of the vortex-tracer system with a very

small time step. A continuous time control algorithm responding to our objective can appear to be complicated to embed on a real tracer given that we are trying to predict the best posterior distribution and *then* steer the sensor to the adequate information rich position. Moreover, any physically controlled system has a response time that is non zero hence asking for a continuous time response can lead to an infinite cost. The data assimilation scheme that we aim to develop will be based on observations collected by an active network of sensors. Information theory comes in handy since we are looking for a set of tools to quantify the amount of information that we can measure from a process. Even though the notions that we will present seem abstract, they make a lot of sense in our application.

We start this section by introducing the discrete version of the system followed by the results of the existing filtering algorithms that we aim to improve. As a start to this climate investigation, we will start with a two point vortex system.

4.2.1 Discrete Problem

We assume that we are only observing the tracers. Their stochastic differential equations depend on the vortices state and hence observing them will convey information about the vortices. The tracers act like a sensor platform. If the observation is made by a Global Positioning System, we can further assume that this observation is precise enough to neglect the noise when we observe the platform position. The observation equation will be exactly $Z_t = (Z_t^1, Z_t^2, \dots, Z_t^N)^T$:

$$Y_{t_k} = Z_{t_k}$$

For the sake of consistency with the usual notations in the filtering problems, we will denote by Z_k the vector position formed by the position of each tracer at time t_k, i.e, $Z_k = (Z_k^{11}, Z_k^{12}, Z_k^{21}, Z_k^{22}, \dots, Z_k^{1N}, Z_k^{2N})^\top$, for N particles.
On the other hand, we can write the stochastic differential equation of the tracers (2.24) and write in the following form:

$$\dot{Z}_t = B(Z_t, X_t)Z_t + C(Z_t, X_t)X_t + \sqrt{2\nu}\eta_t^s, \qquad Z(0) = Z_0 \qquad (4.6)$$

where :

$$B = \frac{1}{2\pi}\begin{pmatrix} \frac{\Gamma_1}{(r_t^{s1})^2} + \frac{\Gamma_2}{(r_t^{s2})^2} & 0 \\ 0 & \frac{\Gamma_1}{(r_t^{s1})^2} + \frac{\Gamma_2}{(r_t^{s2})^2} \end{pmatrix} \tag{4.7}$$

$$C = -\frac{1}{2\pi}\begin{pmatrix} \frac{\Gamma_1}{(r_t^1)^2} & 0 & \frac{\Gamma_2}{(r_t^2)^2} & 0 \\ 0 & \frac{\Gamma_1}{(r_t^1)^2} & 0 & \frac{\Gamma_2}{(r_t^2)^2} \end{pmatrix}$$

Using (4.7), we can write the system equations in a matrix form,

$$\dot{X}_t = A(X_t)X_t + \sqrt{2\nu}\xi_t, \qquad p(X(0) = x) \in (0,1) \tag{4.8}$$

$$\dot{Z}_t^s = B(Z_t, X_t)Z_t^s + C(Z_t, X_t)X_t + \sqrt{2\nu}\eta_t^s, \qquad Z_0^s = Z^s \tag{4.9}$$

where

$$A = \frac{1}{2\pi r_t^2}\begin{pmatrix} -\Gamma_2 & 0 & \Gamma_2 & 0 \\ 0 & -\Gamma_2 & 0 & \Gamma_2 \\ \Gamma_1 & 0 & -\Gamma_1 & 0 \\ 0 & \Gamma_1 & 0 & -\Gamma_1 \end{pmatrix}$$

With this version of the equations of motion (4.8) and (4.9), we can write an elegant discrete version of the nonlinear system,

$$X_{k+1} = X_k + A(X_k)X_k\Delta t + \sqrt{2\nu\Delta t}\xi_k, \quad p(X(k=0) = x) \in (0,1) \tag{4.10}$$

$$Z_{k+1}^s = Z_k^s + \left(B(Z_k, X_k)Z_k^s + C(Z_k, X_k)X_k\right)\Delta t + \sqrt{2\nu\Delta t}\eta_k^s, \quad Z_0^s = Z^s \tag{4.11}$$

Now we will show how one can implement the geometric control developed in Section 4.1 to the discrete system. Even though its application to the objective that we are trying to satisfy, is not very well adapted, we will state the equations as this method can be used for other flowfields. The advantage is that this is applicable in both the deterministic and the stochastic case where the deterministic variables have to be replaced by their expected values.

The control is additive and consists of a turn rate summed to the velocity of the tracers. Recall (4.3), in a complex form, we add $e^{i\theta^s}$ to the velocity which is equivalent to adding a $cos(\theta^s)$ to the first component of the particle

s and $sin(\theta^s)$ to the second component. We can then write the velocity of the tracer s as

$$Z_{k+1}^{1s} = Z_k^{1s} + \left(B(Z_k, X_k)Z_k^s + C(Z_k, X_k)X_k\right)^1 \Delta t + cos(\theta^{1s}) + \sqrt{2\nu\Delta t}\eta_k \tag{4.12}$$

$$Z_{k+1}^{2s} = Z_k^{2s} + \left(B(Z_k, X_k)Z_k^s + C(Z_k, X_k)X_k\right)^2 \Delta t + sin(\theta^{2s}) + \sqrt{2\nu\Delta t}\eta_k \tag{4.13}$$

As a reminder, the superscript $js, j \in \{1, 2\}$, means the component j of the vector associated to the particle s.
To be more accurate, if we examine the time step dependence of the variables between each other, we realize that in discrete time, Z_{k+1} depends on θ_{k-1} since (4.5) is given in terms of $\dot{\gamma}$. Which means that we only dispose of the rate of change of the curvature and that we need to integrate it forward each time step.

We can now complete (4.12) and (4.13) as,

$$Z_{k+1}^{1s} = Z_k^{1s} + \left(B(Z_k, X_k)Z_k^s + C(Z_k, X_k)X_k\right)^1 \Delta t + cos(\theta_{k-1}^{1s}) + \sqrt{2\nu\Delta t}\eta_k 1s \tag{4.14}$$

$$Z_{k+1}^{2s} = Z_k^{2s} + \left(B(Z_k, X_k)Z_k^s + C(Z_k, X_k)X_k\right)^2 \Delta t + sin(\theta_{k-1}^{2s}) + \sqrt{2\nu\Delta t}\eta_k^{2s} \tag{4.15}$$

Equations (4.14) and (4.15) describe the controlled tracer system and the value of θ_k is to be determined. However, the information theoretic cost function formulation presented in section 4.3.2 is not computationally trackable in this form. An alternative formulation is presented below.

In the following, we will examine how we can extract information from the vortices and estimate their position using the position of the tracers. The data assimilation step is performed using nonlinear filtering as well as filtering for linearized systems. The data measured from the position of the tracer are mixed with theoretically propagated states of the vortices to give a more accurate forecast of the flowfield state.

4.2.2 Filtering Algorithms

Linear and nonlinear filtering are very well developed in [23]. The first section of this paper states the fundamental principles. In our case, the information on the state X_k is contained in the observation Z_{k+1}. Filtering in the case of discrete time systems consists of an iterative scheme which output the probability density of the state variable given the measurement received up to that time. We can write this quantity: $p(X_k|Z_{k+1})$, which is called the *posterior* distribution. If we are at time k, we dispose of the following quantities:

- $p(X_k - 1|Z_k)$: *posterior* distribution at time $k-1$
- $p(X_k|X_{k-1})$: which is obtained by propagating the state at time $k-1$ forward in time using the stochastic differential equation (4.10)
- $p(Z_{k+1}|X_k, Z_k)$ which is obtained from the observation equation

Using these well defined quantities, we can calculate the posterior distribution at time k by applying Baye's rule. First, we compute the *prior* density by combining the posterior at the previous time step $k-1$ and the propagation of X_{k-1} forward in time,

$$p(X_k|Z_k) = \int_{X_{k-1}} p(X_k|X_{k-1})p(X_{k-1}|Z_k)dX_{k-1} \tag{4.16}$$

Then, when a measurement is received at time k, we compute the probability density of this measured value given the previous estimated state:

$$p(Z_{k+1}|Z_k, X_k) = \frac{e^{(-\frac{1}{2}(Z_{k+1}-E[Z_{k+1}|Z_k,X_k]))\Sigma^{-1}(Z_{k+1}-E[Z_{k+1}|Z_k,X_k]))^T)}}{\sqrt{2\pi|\Sigma|^{2N}}} \tag{4.17}$$

Combining (4.16) and (4.17), we can write the posterior density which represents the state at the present time including all the available information

using Baye's rule:

$$\begin{aligned} p(X_k|Z_{0:k+1}) &= \frac{p(X_k, Z_{0:k+1})}{p(Z_{0:k+1})} \\ &= \frac{p(X_k, Z_{k+1}, Z_k, Z_{0:k-1})}{p(Z_{0:k+1})} \\ &= \frac{p(Z_{k+1}|Z_k, X_k, Z_{0:k-1})p(Z_k, X_k, Z_{0:k-1})}{p(Z_{0:k+1})} \\ &= \frac{p(Z_{k+1}|Z_k, X_k)p(X_k|Z_{0:k})p(Z_{0:k})}{p(Z_{0:k})} \\ &= \frac{p(Z_{k+1}|Z_k, X_k)p(X_k|Z_{0:k})}{p(Z_{k+1}|Z_{0:k})} \end{aligned}$$

To add more emphasis on the dependence on the control, let us re-write the expression of the posterior distribution taking into account the control variable as a vector $u = (u^1, u^2, \cdots, u^N)$,

$$p(X_k|Z_{0:k+1}, u_{k-1}) = \frac{p(Z_{k+1}|Z_k, X_k, u_{k-1})p(X_k|Z_{0:k})}{p(Z_{k+1}|Z_{0:k}, u_{k-1})}$$

Several filtering algorithms are available in the literature. We commonly talk about Kalman filters and particle filters. For nonlinear systems, the Kalman filter does not apply, that is why extensions that deal with the nonlinearities of the system by using its linearized drift have been developed. In this case we talk about Extended Kalman filter and Ensemble Kalman Filter. We will apply both extended Kalman filtering and particle filtering in order to estimate the position of the vortices given that we only observe the tracers. These sensors are driven by the vortices and thus they contain information about their dynamics. The following are three filtering algorithms that tend to verify existing results since an accurate filtering algorithm is needed to apply the control scheme.

Extended Kalman Filter with deterministic dynamics

The nonlinearities of the dynamical system make it very difficult to estimate. One of the few papers that deal with vortex state estimation claims to use extended Kalman filter and produce an error that tends to zero [24]. We want to verify this result by following the same procedure in order to apply the same algorithm for the control part.

An important point to note is that [24] used a real event simulated in the deterministic case and was applied with only one tracer. Both vortices and tracer did not have noise involved in their dynamics. We now have noise-free observation generated by one simulation of the system. We applied two versions of this filtering algorithm, where the the first version presented follow the stated assumptions whereas in the second (in the next paragraph) we choose to work with a noisy realization as in any filtering problem the true signal is always noisy. Figure 4.3 below is the true signal generated ahead of the filtering with different vortex strenghts (0.5 and 1).

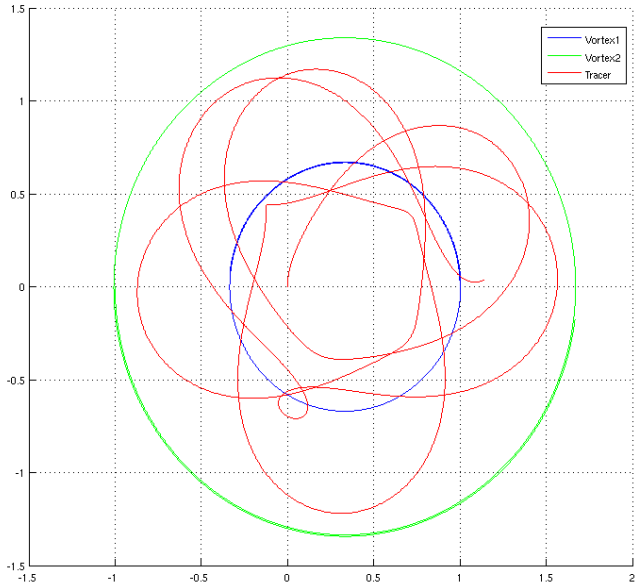

Figure 4.3: True realization: two vortices (different strengths and one tracer)

For the filtering step, we need an observation process driven by noise. For this reason, an artificial noise has to be added to the signals. In addition, we assume that we are able to track the tracers with a Global Positioning System. This makes the noise in the measurements negligible. With this assumption, this algorithm is called a Reduced Extended Kalman Filter (REKF). For the

filtering step we now have,

$$\dot{X}_t^{vortex} = b(X_t^{vortex}) + \sigma_X \dot{W}$$
$$Y = X_t^{tracer}$$

However, since the observations are noise-free, we cannot use them for the filtering. To calculate the innovation in the extended Kalman filter, we will have to take the derivative of Y to get

$$\dot{Y} = \dot{X}_t^{tracer}$$

But $\dot{X}_t^{tracer}$ contains noise as it is given by the noisy tracer equations. This allows us to carry out the usual EKF but using the derivative of the observation in the innovation expression. In fact the observation term used in the innovation is not Y but an increment of Y, or in discrete time $\tilde{Y}_k = Y_{k+1} - Y_k$, which is normally distributed given the vortex state.

Implementing this filtering scheme numerically with one tracer, we get in fact an estimation error that goes to zero as predicted. Figures 4.4 and 4.5 illustrate the estimated position of both vortices as well as the estimation error.

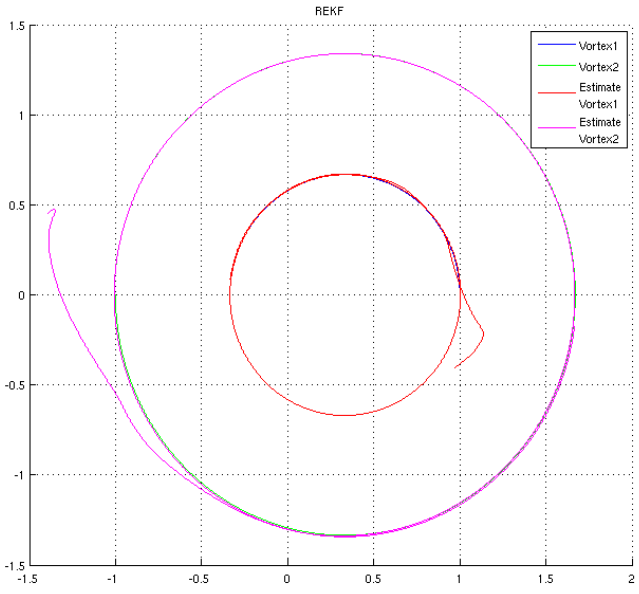

Figure 4.4: Vortex 1 and Vortex 2 estimates vs. true values

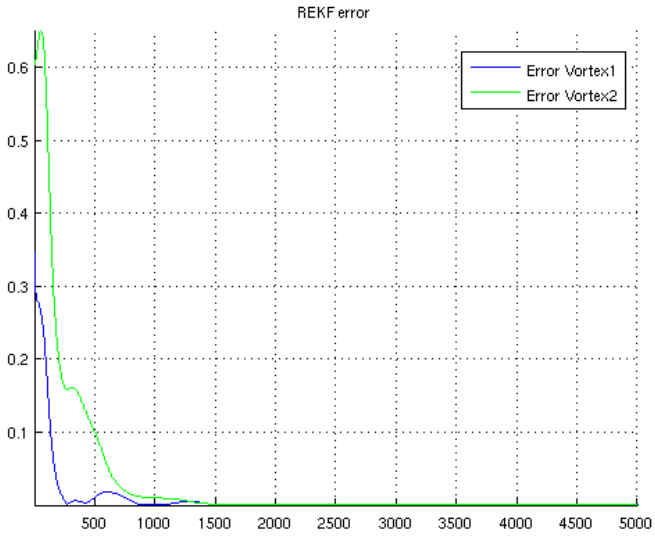

Figure 4.5: Estimation error for Vortex1 and Vortex2

Extended Kalman Filter with random dynamics

After verifying the results found in [24], we would like to apply the same procedure for a real event generated with random dynamics where the noise is additive. The filtering was also carried with an additive noise and the derivative of the position of the tracer was also taken as the innovation. These relaxed assumptions are more common to the filtering audience.
The true signal is plotted in Figure 4.6. As expected, both trajectories of the vortices and tracers are noisy.

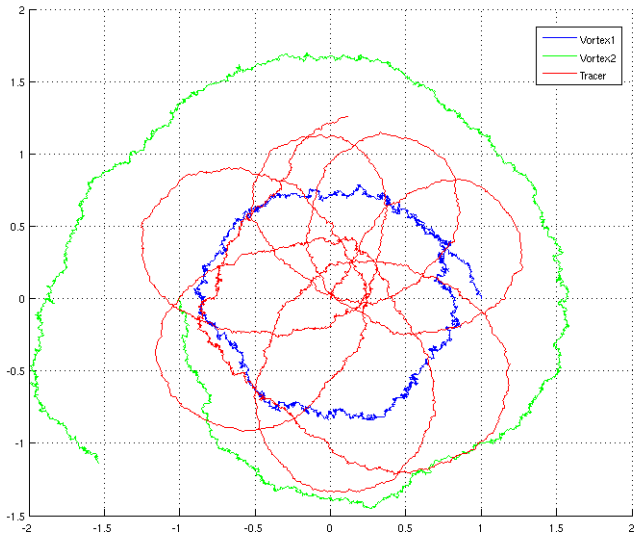

Figure 4.6: True signal with noisy dynamics (Vortex 1, Vortex 2 and Tracer)

We get similar results to the previous algorithm however this time the error is not zero, yet fluctuating near zero with a very small amplitude.
Figures 4.7, 4.8 and 4.9 show the mean values of both vortices position as well as the estimation error in Figure 4.10.

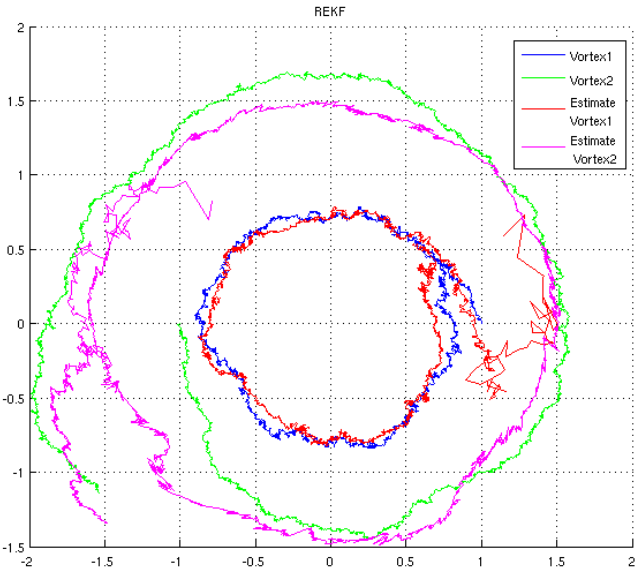

Figure 4.7: Vortex 1 and Vortex 2 estimates vs. true values

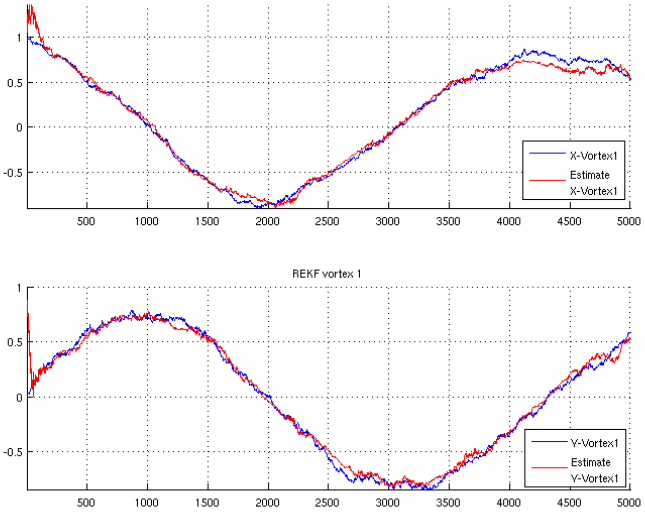

Figure 4.8: Vortex 1 estimates vs. true values

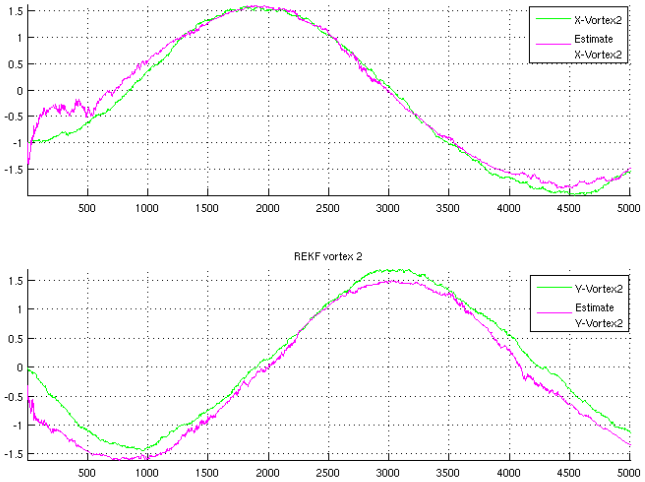

Figure 4.9: Vortex 2 estimates vs. true values

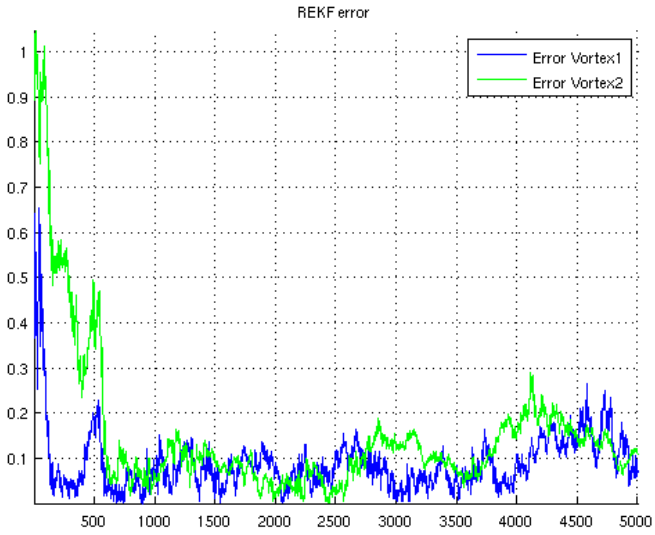

Figure 4.10: Vortex 1 and Vortex 2 estimation errors

Particle Filter

Extended Kalman filter gives a good estimate of the vortex position. However, we can still capture the nonlinearities of the system and relax the assumption on the form of the prior and posterior distribution. This is where particle filters come in handy since we can not only have and estimated state but also a particles representation of the posterior distribution that is not necessarily Gaussian.

As the system is nonlinear, we wanted to see the results produced by a filter more commonly applicable to nonlinear systems that does not require a linearization neither the Jacobian of the system that happens to be quite complicated given the high degree of nonlinearities in the flow dynamics. In addition, particle filtering allows us to avoid taking the derivative of the observation vector in order to have a well defined Riccatti equation.

The real case is simulated using stochastic dynamics, in fact the same as in the previous section and shown in Figure 4.3. The particles represent the vortex position: $\{X_t^p\}_{p=1}^{N_s}$ and the weights are updated using the observation vector, which is nothing but the tracer dynamics but in a hybrid way. Indeed, we calculate the tracer position that is created by the particle p using the previous "real" observation since it is available to us. Discretizing the tracer

dynamics leads to:

$$Y_k = Y_{k-1} + h(X_{k-1}, Y_{k-1})\Delta t + \sigma_Y \sqrt{\Delta t}\Delta V$$

In order to obtain the observation created by the particle p, we compute:

$$Y_k^p = Y_{k-1} + h(X_{k-1}^p, Y_{k-1})\Delta t + \sigma_Y \sqrt{\Delta t}\Delta V$$

and the weights update would be based on $Y_k - Y_k^p$.
The results of the simulations are given in Figures 4.11, 4.12, 4.13 and 4.14 and we obtain a good estimate that seems to be more accurate than the one found in [2].

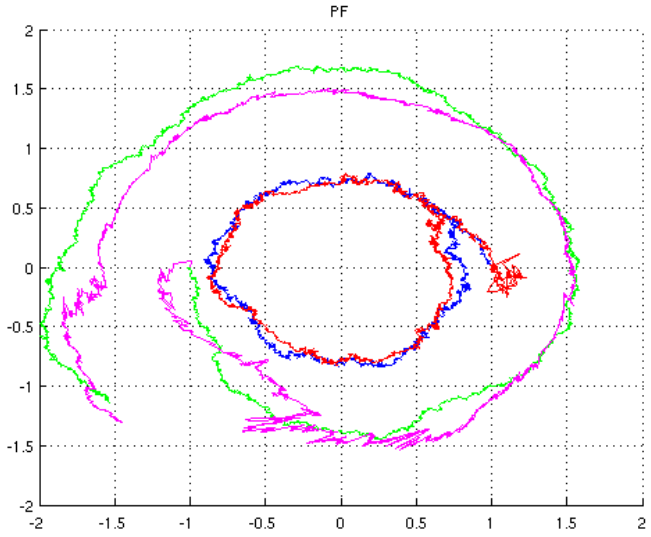

Figure 4.11: Vortex 1 and Vortex 2 estimates vs. true values

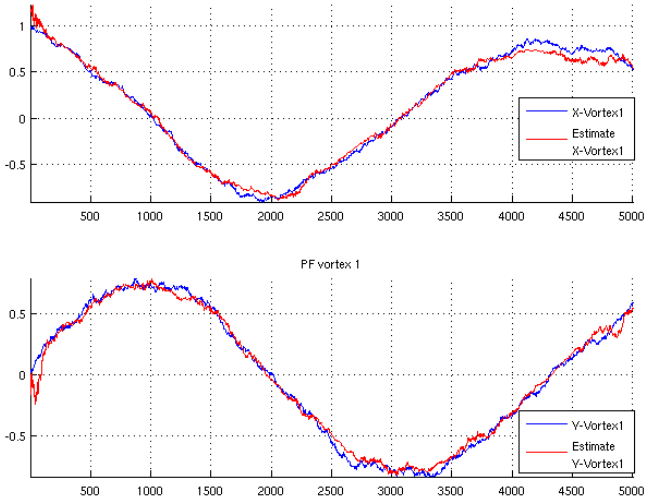

Figure 4.12: Vortex 1 estimate vs. true value

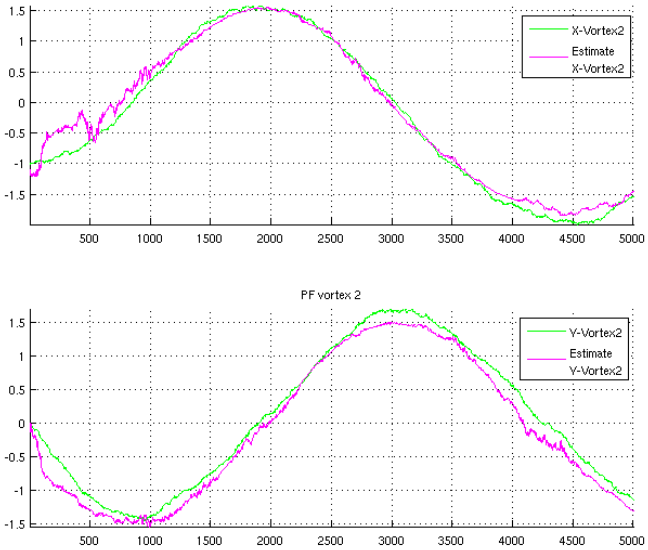

Figure 4.13: Vortex 1 estimate vs. true value

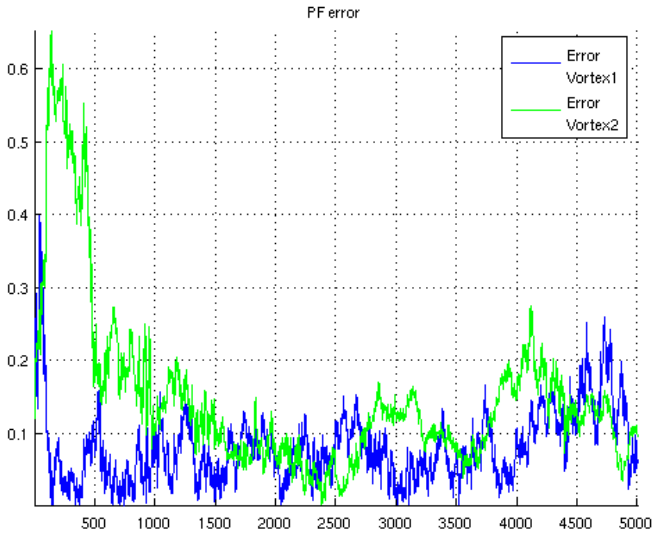

Figure 4.14: Estimation Error in Vortex 1 and Vortex 2

Ensemble Kalman Filter

A good compromise between Extended Kalman filter and Particle filter is the Ensemble Kalman filter (EnKF). The reader is referred to [22] for further details on the algorithm steps. The general idea is to represent the conditional state distribution by an ensemble of particles and assume that this distribution is gaussian and obtain its mean and variance by taking the mean and the variance of the position of the particles. We apply the EnKF to the realization of 4.3. The results are shown is Figure 4.15, 4.16, 4.17 and 4.18.

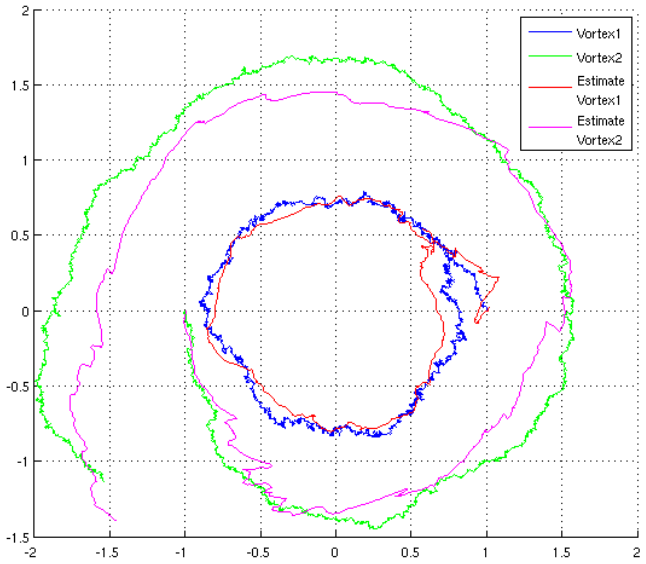

Figure 4.15: Vortex 1 and Vortex 2 estimates vs. true values

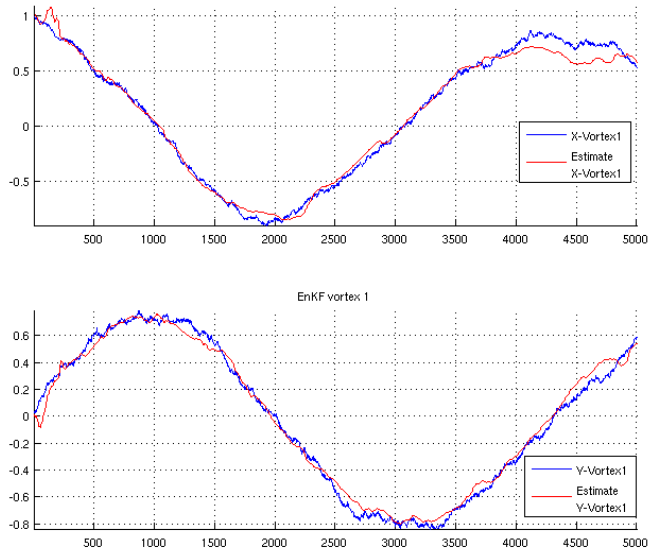

Figure 4.16: Vortex 1 estimates vs. true values

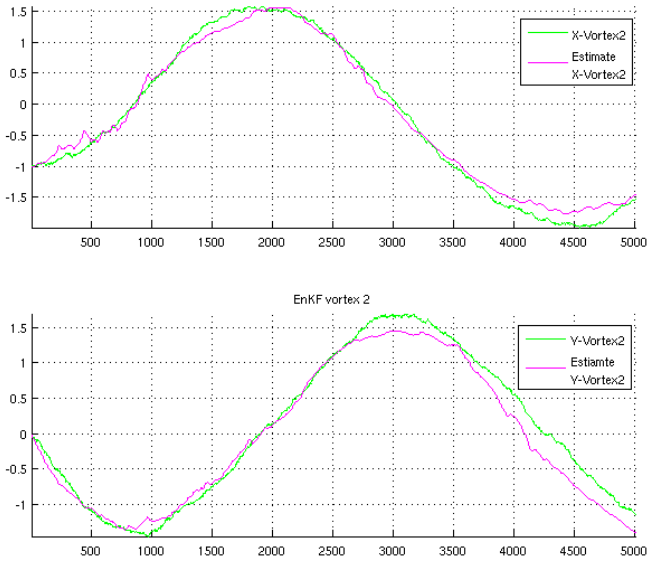

Figure 4.17: Vortex 1 estimates vs. true values

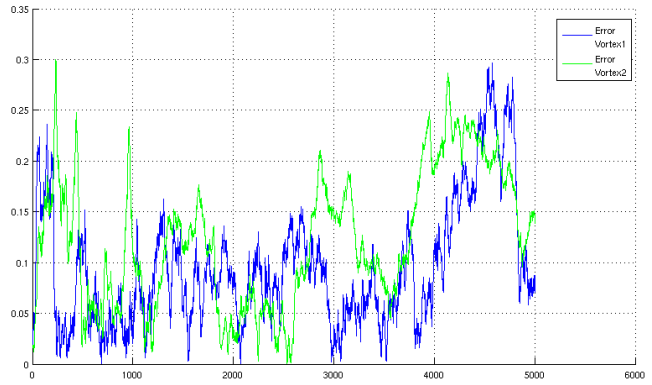

Figure 4.18: Vortex 1 estimates vs. true values

In the following we show how to get the control variable u in order to satisfy our objective to collect useful information. We will define what we mean by "useful" and design a cost function that takes into account the state vectors as well as a measure of information.

4.3 Information Theory Based Control

4.3.1 Information Theory Background

Some background on information theory is needed to fully understand why this brings very powerful tools to probability theory and control theory. As we saw in equation (4.3), the only missing parameter is the prescribed center. We want that prescribed center to be the one containing the most useful information in the two dimensional space at the time of the measurement. However, since we are trying to determine that location before actually getting the measurement, we will look for the location in the space that is *expected* to give the best information. How to quantify the amount of information present in a certain location? How to compare it with information from another location? How to measure the uncertainty in a certain state variable? etc, are all questions that information theory can answer. Let us first start by stating definitions of important information theory measure.

Definition 4.3.1. ***Entropy (Shannon Entropy)*** *Physically, the entropy measures the uncertainty in the outcome of an experiment. It also quantifies the average amount of information needed to describe a random variable. We define the entropy H as measure of a set of probabilities $P = (p_1, p_2, \cdots, p_n)$ for all possible events and it is given by [27]:*

$$H(P) = -\sum_{i=1}^{n} p_i log(p_i) \quad if\ discrete$$

$$H(P) = -\int_x p_(x) log(p(x)) \quad if\ continuous$$

for example, for a n-dimensional normal distribution $p = N(\mu, \Sigma)$, $H = \frac{1}{2}\log((2\pi e)^n|\Sigma|)$.

Next, we define the divergence between two probability densities. We can think about it as a distance in the probability space even though it is not symmetric and does not satisfy the triangular inequality.

Definition 4.3.2. ***Kullback Leibler Divergence*** *It is the most used divergence in information theory since it has a very nice expression and appears naturally in multiple problems. The Kullback Leibler measures the difference*

between two densities p and q. In other words, it is the error made in assuming a certain distribution q on a random variable when the true distribution is p. Mathematically it is given by,

$$D[p||q] = \sum_x p(x) log\left(\frac{p(x)}{q(x)}\right)$$

The last very important quantity that we shall define is the Information Gain.

Definition 4.3.3. ***Information Gain (Mutual Information)*** *It represents the reduction of entropy in one random variable due to another random variable. It also measures the dependence between two random variables.*

$$I(X;Y) = H(X) - H(X|Y)$$

4.3.2 Control Objective and Cost Function

For the control problem, the objective is to take the measurement that maximizes the amount of information that we expect to have on the vortices state. Since the measurements are equivalent to the tracer position, we can state this objective differently by seeking the position in the space that will contain the best information and will reduce the amount of uncertainty that we have on the state random variable, i.e., the vortex position.
From a filtering point of view, we translate this objective by maximizing some sort of distance between the prior and posterior densities. This distance is dependent on the future observation that we aim to make optimal. This observation is not available yet hence it needs to be averaged out.
We can now define mathematically this cost function using Section 4.3.1 as follows,

$$J[u_{k-1}] = \int_{Z_{k+1}} D[p(X_k|Z_{k+1}, u_{k-1})||p(X_k|Z_k)]p(Z_{k+1}|Z_k, u_{k-1})dZ_{k+1} \quad (4.18)$$

The control that we will apply is the one that maximizes J.
We want to maximize the distance between the prior and posterior density and average it over all possible observations at the next time step. Indeed, the Kullback Leibler distance is an integral over the vortex state. Hence in

$D[p(X_k|Z_{0:k+1}, u_{k-1})||p(X_k|Z_{0:k})]$, Z_{k+1} is unknown since it is not received yet.

Some manipulations on (4.18) lead to,

$$\begin{aligned}
J[u_{k-1}] &= \int_{Z_{k+1}} D[p(X_k|Z_{k+1}, u_{k-1})||p(X_k|Z_k)]p(Z_{k+1}|Z_k, u_{k-1})dZ_{k+1} \\
&= \int_{Z_{k+1}} \left(\int_{X_k} p(X_k|Z_{k+1}, u_{k-1}) \log \left(\frac{p(X_k|Z_{k+1}, u_{k-1})}{p(X_k|Z_k)} \right) dX_k \right) \\
&\times p(Z_{k+1}|Z_k, u_{k-1})dZ_{k+1} \\
&= \int_{Z_{k+1}} \int_{X_k} \frac{p(X_k, Z_{k+1}|Z_k, u_{k-1})}{p(Z_{k+1}|Z_k, u_{k-1})} \log \left(\frac{p(X_k, Z_{k+1}|Z_k, u_{k-1})}{p(Z_{k+1}|Z_k, u_{k-1})p(X_k|Z_k)} \right) \\
&\times p(Z_{k+1}|Z_k, u_{k-1})dX_k dZ_{k+1} \\
&= \int_{Z_{k+1}} \int_{X_k} p(X_k, Z_{k+1}|Z_k, u_{k-1}) \log \left(\frac{p(X_k, Z_{k+1}|Z_k, u_{k-1})}{p(Z_{k+1}|Z_k, u_{k-1})p(X_k|Z_k)} \right) \\
&\times dX_k dZ_{k+1} \\
&= I[p(X_k|Z_{k+1}, u_{k-1})||p(X_k|Z_k)] \\
&= I(X_k; X_k|Z_{k+1}) \qquad (4.19)
\end{aligned}$$

This explains why we are looking for the value of u that maximizes J so that the expected measurement at the next time step reduces the uncertainty on X since the Information Gain quantifies the reduction in entropy.
Furthermore, given the definition of the information gain, maximizing (4.19) is equivalent to minimizing the conditional entropy.

From an analytical point of view, the densities involved in the cost function cannot be obtained explicitly due to the double integral. Also, even if we take the derivative and equate it to zero then try to solve for the control, it would be impossible to extract u analytically.
To obtain an approximations on the control needed to steer the tracer, a possible solution is to work with linearized equations in the optimization step. In this case, we know that the posterior distribution is gaussian with mean and covariance given by the Kalman filter. Furthermore, we recall that our objective is equivalent to minimizing the conditional entropy, which is also equivalent to minimizing the determinant or the covariance matrix of the posterior distribution in the case of a linear system. We will make use of the Extended Kalman filter where the covariance is given by the Riccati

equation. In this case, the observation equation will be taken as

$$Y_k = Z_k - Z_{k-1} \tag{4.20}$$

On the other hand, we linearize the equations of motion around the previous expected value of the vortex position which is a known value to us at the current time step.
A very important point to note is that the linear system is only used when the control parameter is determined. After this step, we will use the nonlinear form of the drift and sensor function as well as the control determined by the linear set up.
We will do the following analysis in discrete time as it is much more straight forward to think in terms of time steps. The system equations will be:

$$\begin{aligned} X_k &= X_{k-1} + \Delta t(F_{k-1}X_{k-1}) + \sigma_X \Delta W_k \\ Y_k &= \Delta t(H_{k-1}X_{k-1} + u_{k-1}) + \sigma_Y \Delta V_k \end{aligned} \tag{4.21}$$

where $F_{k-1} = \frac{\partial f}{\partial X}\Big|_{\hat{X}_{k-1}}$ and $H_{k-1} = \frac{\partial h}{\partial X}\Big|_{\hat{X}_{k-1}, y_{k-1}}$.

The first control strategy that one can think of is linear feedback control. In the case of a linear system with white gaussian noise, the cost function (4.19) is given by:

$$I[X_k|Y_k^c] = H(X_k) - H(X_k|Y_k^c) \tag{4.22}$$

We insist on the fact that the control is contained in the observation Y_k by adding the superscript c. Now recall the REKF equations:

$$\begin{aligned} \hat{x}_{k|k-1} &= b(\hat{x}_{k-1|k-1}, u_{k-1}) \\ P_{k|k-1} &= F_{k-1}P_{k-1|k-1}F_{k-1}^T + Q_{k-1} \\ \tilde{y}_k &= y_k - h(\hat{x}_{k|k-1}) \\ S_k &= H_k P_{k|k-1} H_k^T + R_k \\ K_k &= P_{k|k-1} H_k^T S_k^{-1} \\ \hat{x}_{k|k} &= \hat{x}_{k|k-1} + K_k \tilde{y}_k \\ P_{k|k} &= (I - K_k H_k) P_{k|k-1} \end{aligned}$$

where Q_k and R_k are the covariances of the noise in the state and observation equation, respectively.
In this case, we can write (4.22) as:

$$I[X_k; Y_k] = \frac{1}{2} log((2\pi e)^4 |P_{k|k-1}|) - \frac{1}{2} log((2\pi e)^4 |P_{k|k}|) \tag{4.23}$$

If we had a linear feedback control, (4.21) becomes:

$$Y_k = \Delta t(H_{k-1} X_{k-1} + C X_{k-1}) + \sigma_Y \Delta V_k \tag{4.24}$$

Writing $u_{k-1} = C X_{k-1}$ would not make sense since we do not have the value of X_{k-1} but only its expected value. The tracer only knows the matrix H hence C has to be proportional to H. Let us write the feedback control parameter as

$$C = \Theta H \tag{4.25}$$

The observation equation (4.24) can be written as

$$\begin{aligned} Y_k &= \Delta t((H_{k-1} + \Theta_{k-1} H_{k-1}) X_{k-1}) + \sigma_Y \Delta V_k & (4.26)\\ &= \Delta t(I + \Theta_{k-1}) H_{k-1} X_{k-1} + \sigma_Y \Delta V_k & (4.27) \end{aligned}$$

Since we do not impose any restriction on Θ, let us define $\tilde{\Theta} = I + \Theta$ and $\tilde{\Theta} H$ can actually be any matrix of adequate size.

Now, we would like to determine C such that (4.23) is maximized. This is equivalent to finding C that minimizes $log((2\pi e)^4 |P_{k|k}|)$.
Re-writing the filter equations depending on the control, we have:

$$\begin{aligned} \hat{X}_{k|k-1} &= b(\hat{X}_{k-1|k-1}, u_{k-1}) \\ P_{k|k-1} &= F_{k-1} P_{k-1|k-1} F_{k-1}^T + Q_{k-1} \\ \tilde{y}_k &= y_k - h(\hat{X}_{k|k-1}) \\ S_k &= \tilde{\Theta}_k H_k P_{k|k-1} H_k^T \tilde{\Theta}_k^T + R_k \\ K_k &= P_{k|k-1} H_k^T \tilde{\Theta}_k^T S_k^{-1} \\ \hat{x}_{k|k} &= \hat{x}_{k|k-1} + K_k \tilde{y}_k \\ P_{k|k} &= (I - K_k \tilde{\Theta}_k H_k) P_{k|k-1}. \end{aligned}$$

On the other hand, we can translate this algorithm in continuous time since in a real system, the dynamics would be continuous. The Extended Kalman filter in continuous time is,

$$\frac{d\hat{X}}{dt} = F_t\hat{X}_t + K_t(Y_t - \tilde{\Theta}_t H_t \hat{X}_t) \tag{4.28}$$

$$K_t = P_t H_t^T \tilde{\Theta}_t^T R^{-1} \tag{4.29}$$

$$\frac{dP}{dt} = F_t P_t + P_t F_t^T + Q - K_t R K_t^T \tag{4.30}$$

We simulate (4.30) using an Euler scheme we have a propagation equation for the covariance matrix that can be written as:

$$P_k = P_{k-1} + \Delta t(F_{k-1}P_{k-1} + P_{k-1}F_{k-1}^T + Q - K_{k-1}RK_{k-1}^T) \tag{4.31}$$

$$= P_{k-1} + \Delta t(F_{k-1}P_{k-1} + P_{k-1}F_{k-1}^T + Q - K_{k-1}RK_{k-1}^T) \tag{4.32}$$

To summarize this set up, maximizing the information gain between the prior and posterior is equivalent to finding $\tilde{\Theta}$ such that

$$\tilde{\Theta} = \underset{\tilde{\Theta}}{\operatorname{argmin}}\ log((2\pi e)^4 |P_k(\tilde{\Theta})|) \tag{4.33}$$

4.4 Results

Every result obtained used the control algorithm will be compared to an estimation using the REKF without control.

For a a certain realization, the REKF gives the following results where (4.19) represents the estimation of both coordinates of Vortex 1, (4.20) the estimation of both coordinates of Vortex 2 and (4.21) the estimation error of both vortices.

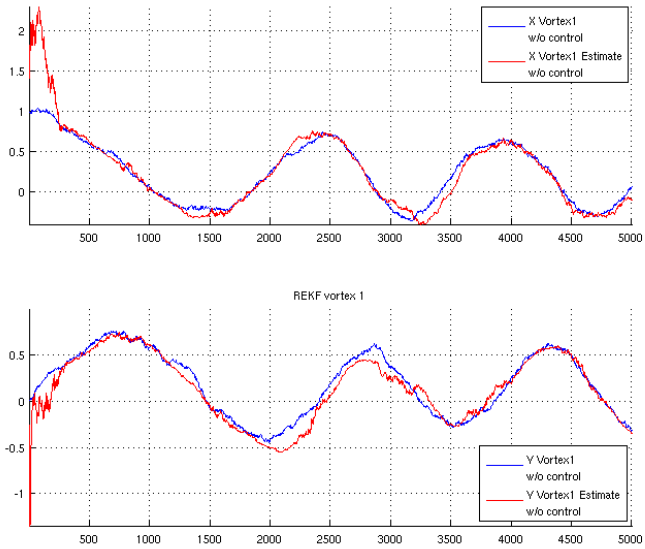

Figure 4.19: Vortex 1 estimates vs. true values

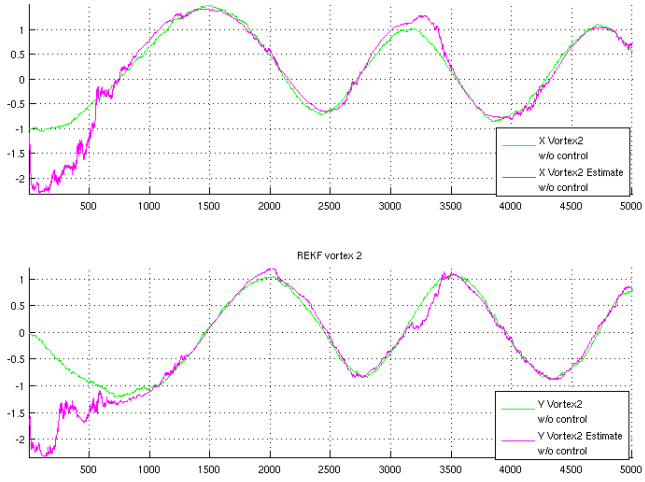

Figure 4.20: Vortex 2 estimates vs. true values

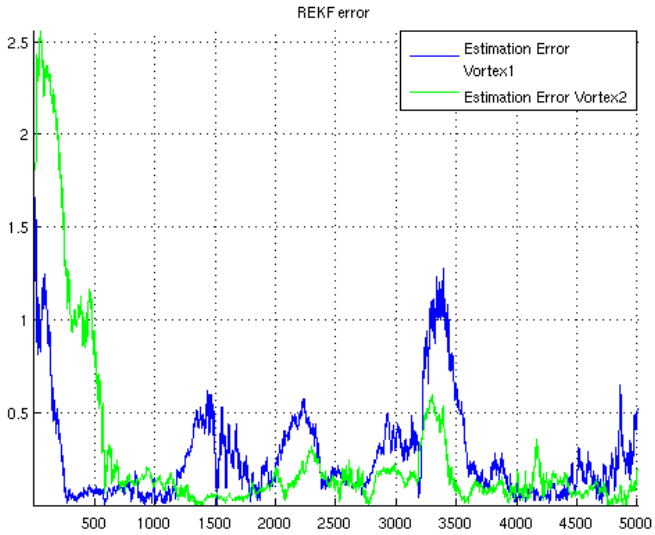

Figure 4.21: Estimation Error for Vortex 1 and Vortex 2

The total average estimation error in this case is 52%. This value is the sum of the relative error in the estimation of Vortex 1 and Vortex 2. Even though there is not a lot of room for improvement, the results of our algorithm below show a reduction in the relative total average error as well as a reduction in the uncertainty that governs the vortex state through a reduction in its entropy.

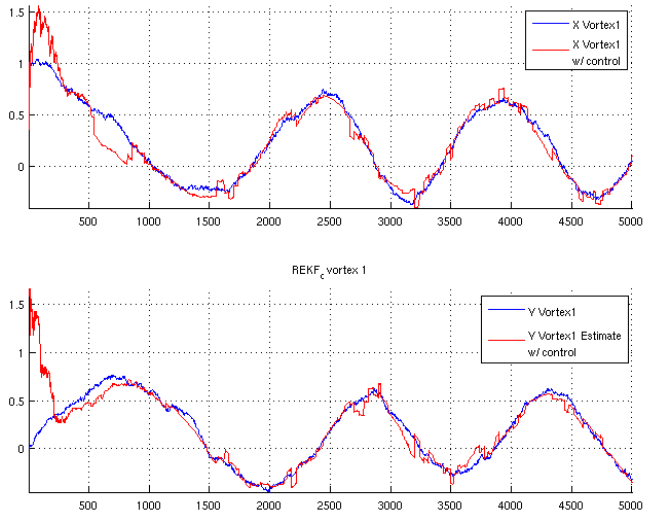

Figure 4.22: Vortex 1 estimates w/ control vs. true values

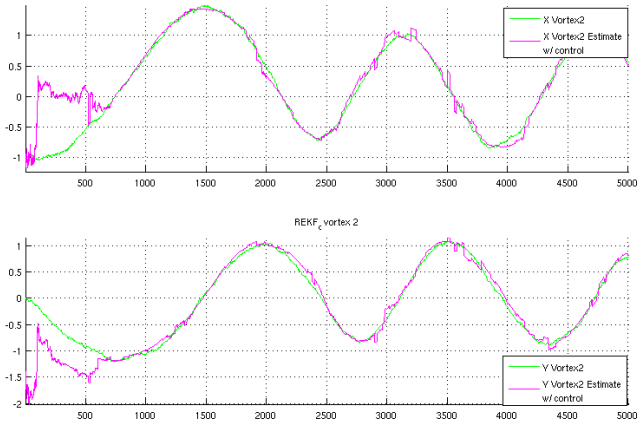

Figure 4.23: Vortex 2 estimates w/ control vs. true values

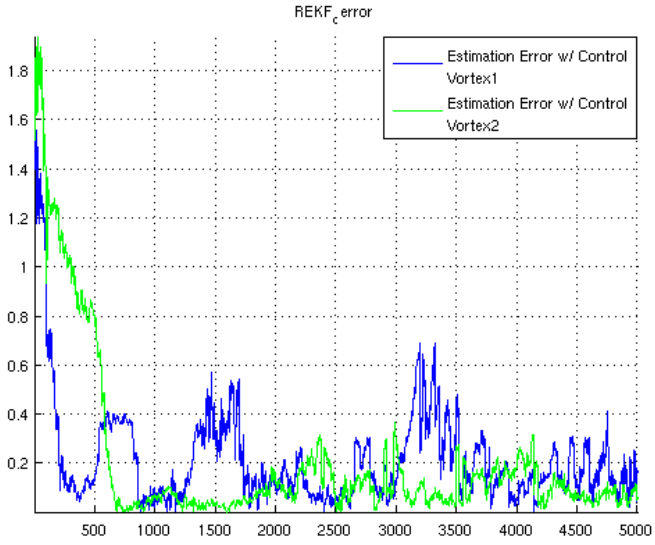

Figure 4.24: Estimation Error w/ control for Vortex 1 and Vortex 2

The figure below compares the entropy $H(X|Y)$ for the estimation with and without control. We had to impose a threshold on the entropy with control: the optimization step is performed at each time step of the integration and it happens that the control parameters are non zero for each evaluation. This can lead to a control variable that dominates the dynamics of the tracer and the steering command may not be feasible in one time step.
The average total estimation error drops to 42% in this case and the reduction in error is 10%.

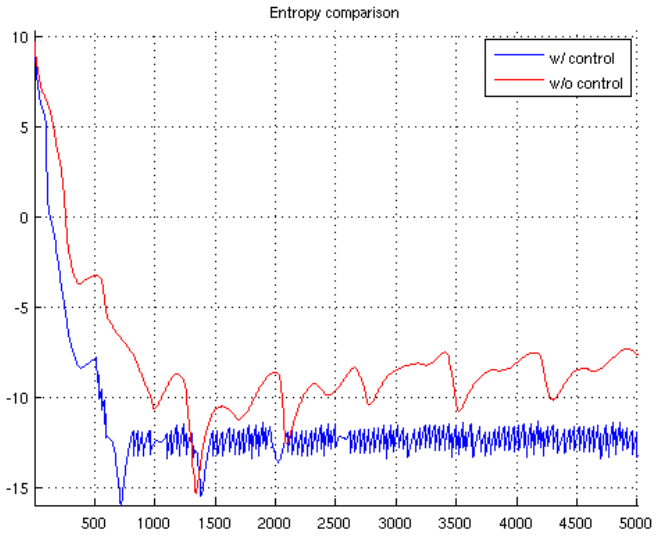

Figure 4.25: Entropy comparison

These simulations were performed with a covariance noise of $\sigma = 0.001$ and control parameter evaluated at each time step. Hence to check the robustness of our algorithm with respect to the noise amplitude as well as the initial covariance, we carry the simulation again this time a noise covariance of $\sigma = 0.005$. We obtain results very similar to the ones above. The estimation is very accurate and we realize a significant reduction in the conditional entropy. The figures below show the realizations used as well as a comparison of the estimation when the control algorithm is used and not used.

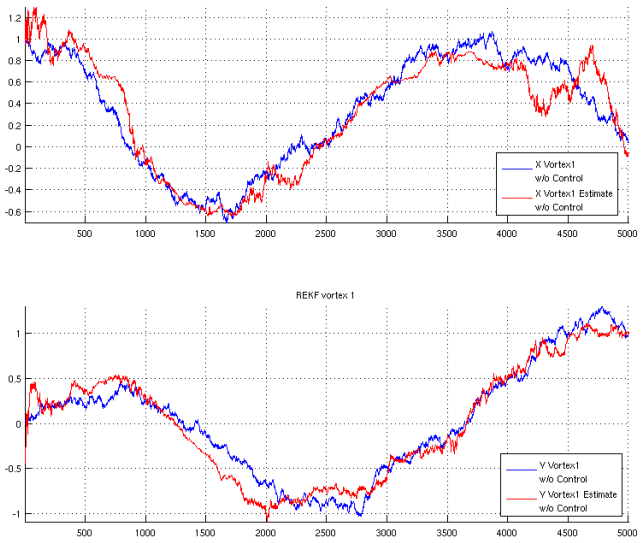

Figure 4.26: Vortex 1 estimates ($\sigma = 0.005$) vs. true values

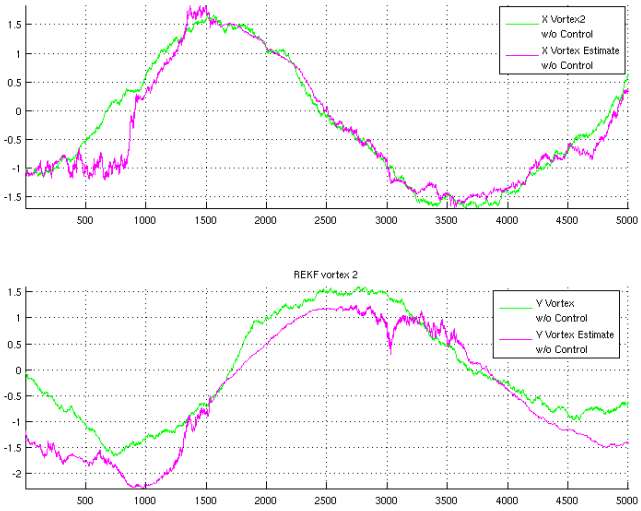

Figure 4.27: Vortex 2 estimates ($\sigma = 0.005$) vs. true values

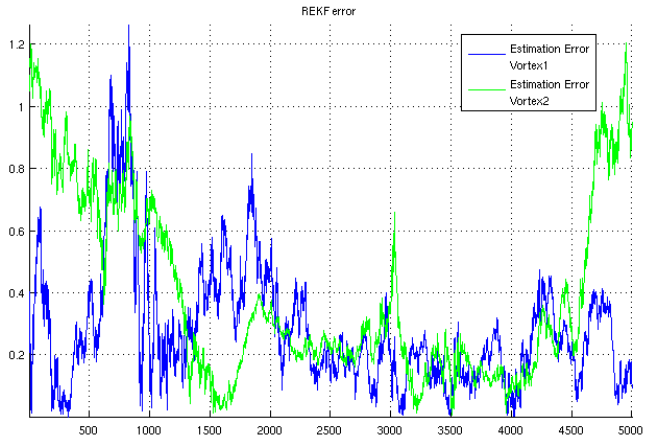

Figure 4.28: Estimation error for $\sigma = 0.005$ (w/o control)

Applying the control we have,

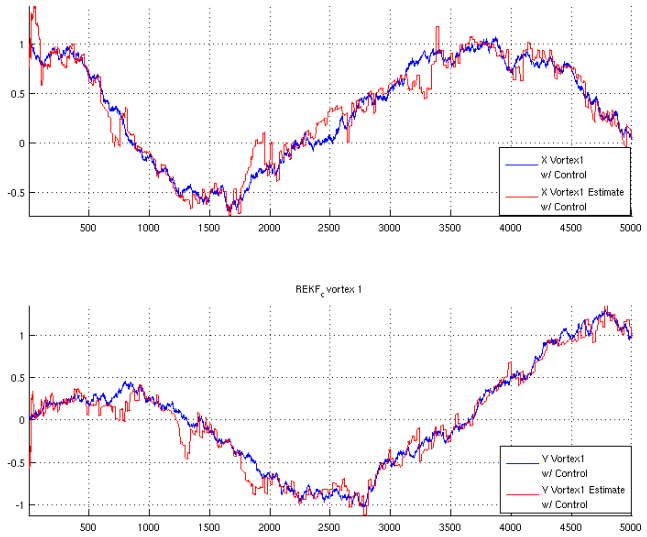

Figure 4.29: Vortex 1 estimates w/ control ($\sigma = 0.005$) vs. true values

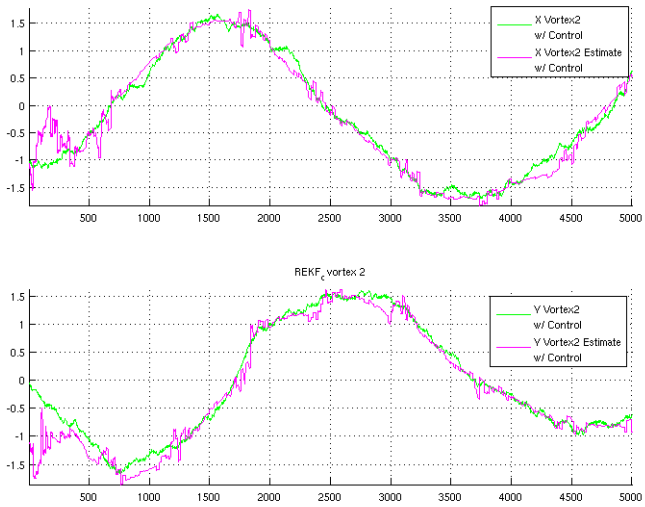

Figure 4.30: Vortex 2 estimates w/ control ($\sigma = 0.005$) vs. true values

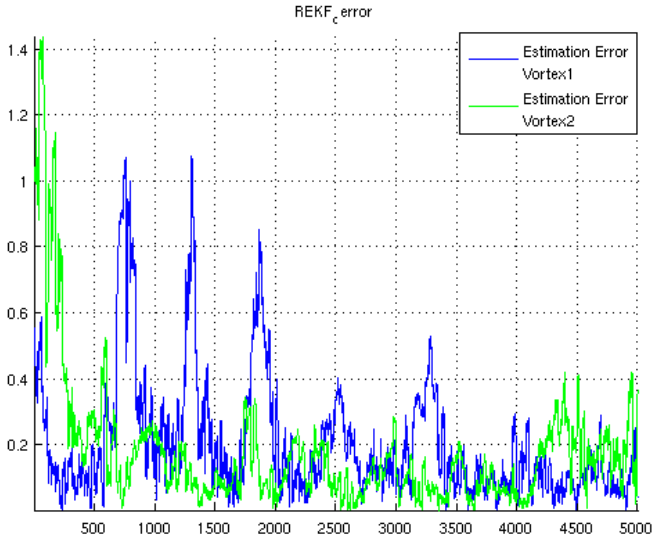

Figure 4.31: Estimations errors w/ control for $\sigma = 0.005$

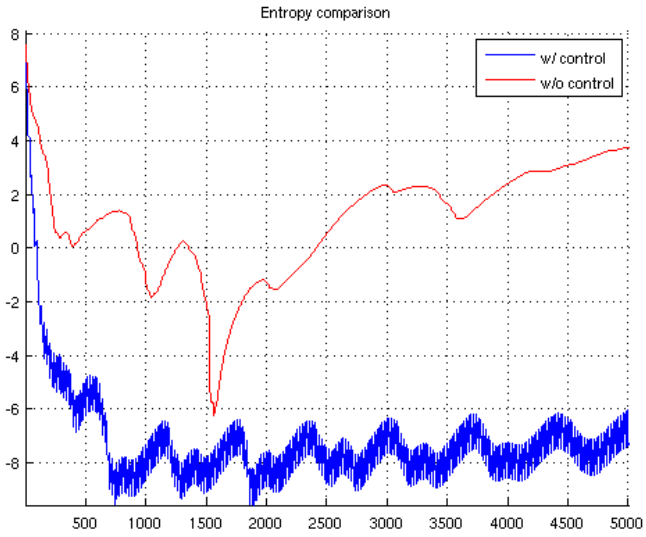

Figure 4.32: Entropy comparison for $\sigma = 0.005$

The improvement in the estimation accuracy is not clear from the plots given small value of the error when no control is applied. However, computing its total relative average show a reduction of 12% in the estimation error.

During the simulations, we also encountered the case where the initial conditions led to a divergence in the filtering without control. The initial condition was in the non-observable subspace. Figures 4.33, 4.34 and 4.35 are for estimation without control where we clearly see that the REKF fails to estimate the vortex state when the noise covariance is high, ie. $\sigma = 0.005$.

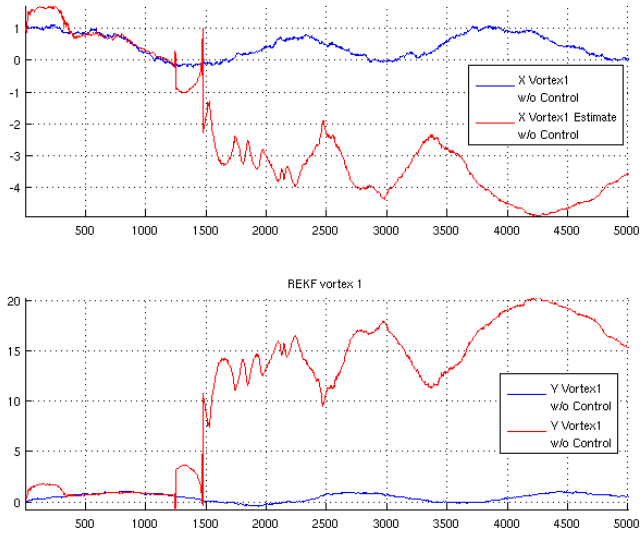

Figure 4.33: Vortex 1 estimates w/o control ($\sigma = 0.005$) vs. true values

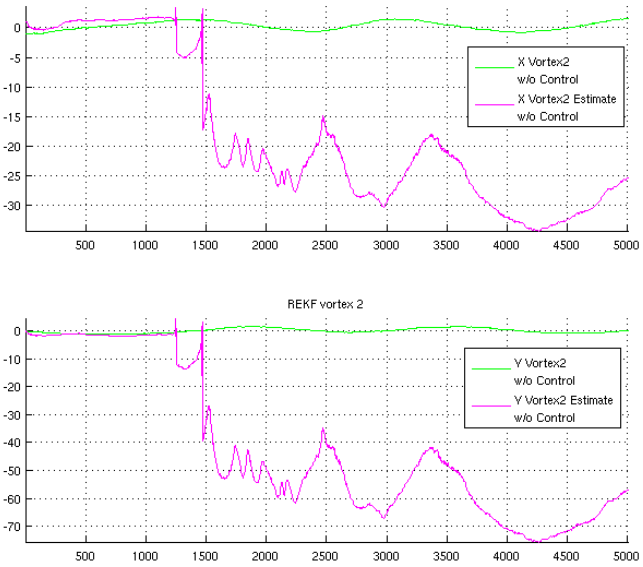

Figure 4.34: Vortex 2 estimates w/o control ($\sigma = 0.005$) vs. true values

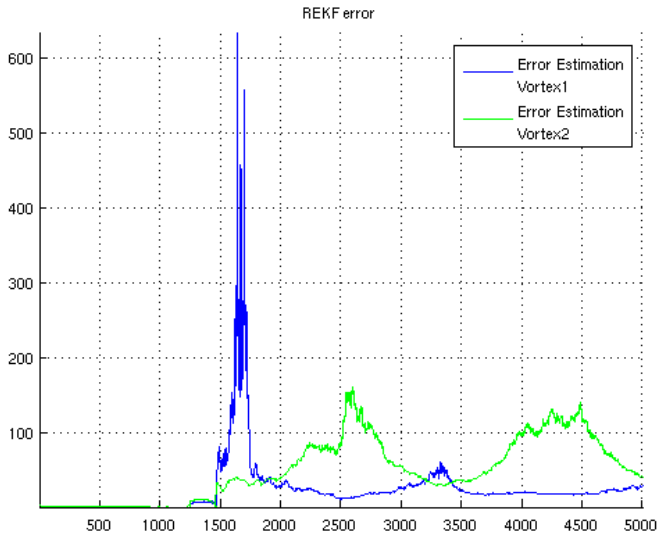

Figure 4.35: Estimation error w/ control ($\sigma = 0.005$)

The filtering performed with our control scheme, succeed in the estimation and it tracks with a low error the true state. Figures 4.36, 4.37 and 4.38 show the filtering performance with control.

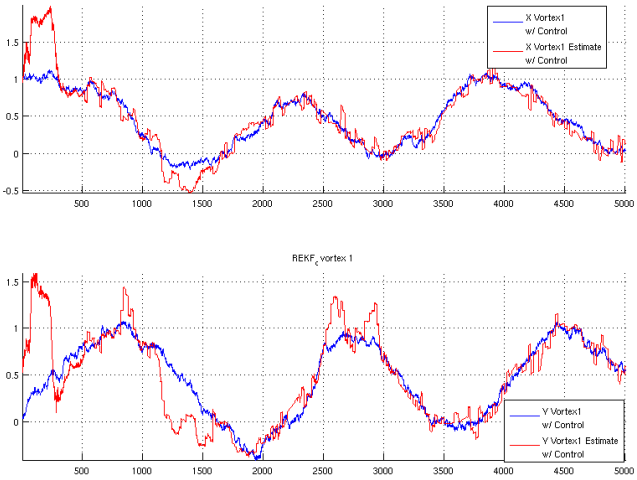

Figure 4.36: Vortex 1 estimates w/ control ($\sigma = 0.005$) vs. true values

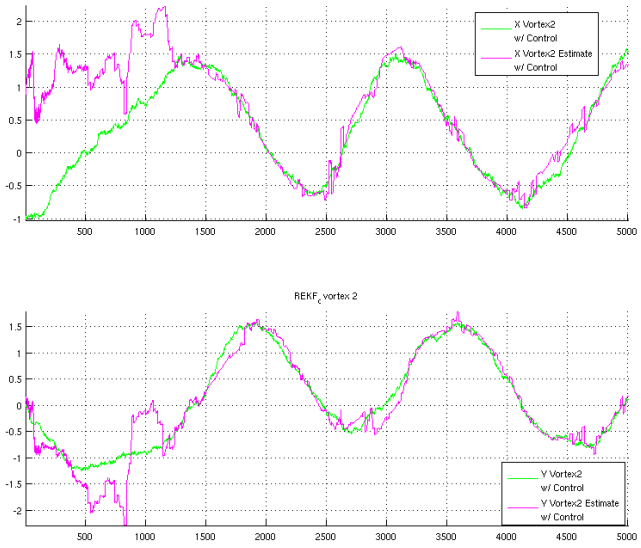

Figure 4.37: Vortex 2 estimates w/ control ($\sigma = 0.005$) vs. true values

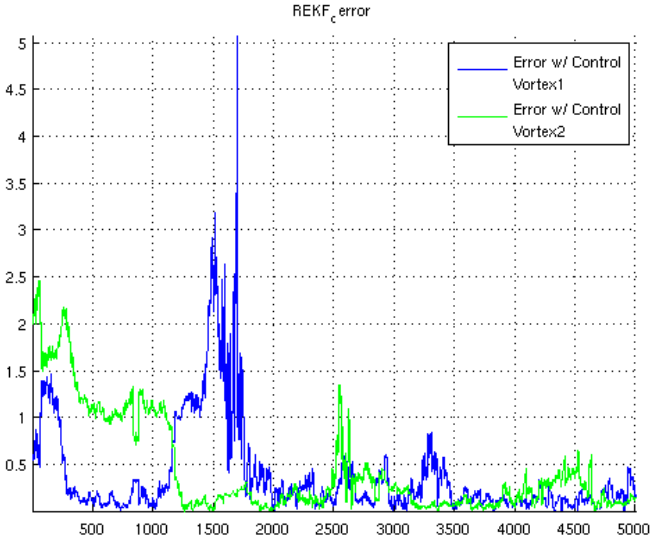

Figure 4.38: Estimation error w/ control ($\sigma = 0.005$)

The entropy stays under control as well and does not blow up as shown in Figure 4.39.

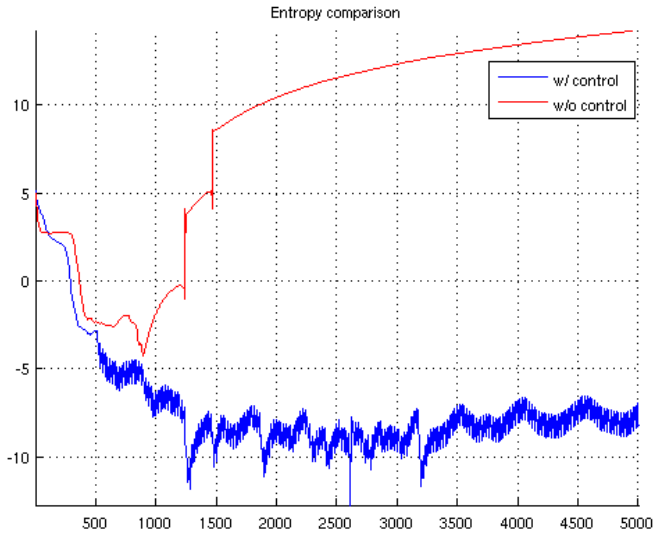

Figure 4.39: Entropy comparison w/ control ($\sigma = 0.005$)

4.4.1 Results Validation

To verify these results, we perform a statistical study by running the algorithm multiple times. Indeed, we run 40 realizations and perform the estimation with and without control 40 times for each realization. The tables below contain the average error as well as the average entropy for both cases with and without control. The columns "Relevant Experiments" represents the number of experiments that were used in the average where we drop the experiments that blow up.

On average, the error for the estimation with control is smaller by 6.6 % and the Entropy is smaller by 4 units.

On average, our algorithm performs better than a standard REKF. Furthermore, it is more robust to "wild" initial conditions that can make the estimation blow up or inaccurate enough.

Table 4.1: Average Error and Relevant Experiments for $\sigma = .001$

Average Error_C %	Relevant Experiments_C	Average Error %	Relevant Experiments
0.21058	40	0.27851	40
0.22299	38	0.28964	39
0.20289	37	0.28382	40
0.20704	39	0.27536	39
0.23998	38	0.29236	40
0.20814	35	0.26278	40
0.215	40	0.28585	40
0.20906	36	0.29131	39
0.22658	40	0.295	40
0.20628	39	0.27802	40
0.20659	40	0.28533	40
0.21911	38	0.28108	39
0.20889	39	0.28323	37
0.21651	36	0.27405	40
0.22805	36	0.3121	40
0.21754	38	0.29855	38
0.2295	38	0.28876	40
0.2197	39	0.27676	40
0.22406	38	0.29443	40
0.21397	40	0.2786	39
0.22019	40	0.28204	40
0.22481	38	0.28942	40
0.21981	40	0.2804	40
0.21327	40	0.28718	39
0.21596	37	0.27074	40
0.22988	39	0.31762	40
0.22152	40	0.28307	40
0.20855	40	0.27158	40
0.22453	39	0.28054	40
0.22557	38	0.29335	38
0.20887	38	0.27334	40
0.23937	39	0.28729	39
0.2284	39	0.29024	40
0.20808	40	0.27014	39
0.21947	40	0.27888	39
0.21073	40	0.27336	40
0.1998	38	0.26704	40
0.2285	39	0.3043	39
0.21075	40	0.27924	40
0.21973	38	0.28986	39

Table 4.2: Average Entropy and Relevant Experiments for $\sigma = .001$

Average Entropy_C %	Relevant Experiments_C	Average Entropy %	Relevant Experiments
-12.656	40	-8.7471	40
-12.294	40	-8.5085	40
-12.091	40	-8.6406	40
-12.361	40	-7.0734	40
-12.237	40	-8.8276	40
-11.709	40	-8.5234	40
-12.672	40	-8.6205	40
-11.895	40	-7.2191	40
-12.654	40	-8.6979	40
-12.425	40	-8.8271	40
-12.658	40	-8.6979	40
-11.607	40	-8.7244	40
-12.38	40	-6.1113	40
-11.967	40	-8.7362	40
-11.86	40	-8.8551	40
-11.994	40	-7.0829	40
-12.136	40	-8.8584	40
-12.668	40	-8.8138	40
-12.02	40	-8.8175	40
-12.664	40	-7.7197	40
-12.677	40	-8.817	40
-12.11	40	-8.6554	40
-12.656	40	-8.8393	40
-12.664	40	-7.4851	40
-11.78	40	-8.7026	40
-12.385	40	-8.7524	40
-12.664	40	-9.0714	40
-12.669	40	-8.6983	40
-12.329	40	-8.8179	40
-12.09	40	-6.7133	40
-12.143	40	-8.8436	40
-12.35	40	-7.9954	40
-12.319	40	-8.9375	40
-12.67	40	-7.2366	40
-12.662	40	-7.541	40
-12.647	40	-8.87	40
-12.056	40	-8.6676	40
-12.401	40	-8.654	40
-12.651	40	-8.7118	40
-12.303	40	-8.6752	40

CHAPTER 5

CONCLUSION

The purpose of this thesis was to introduce a novel data assimilation method that blends classical filtering algorithms and a controlled platform of sensors. The control objective was to steer this platform to information rich locations in the space. Chapter 2 presented the system to which we applied the said algorithm. We derived the equations of motion of a flowfield formed by N vortices observed by a set of UAVs. This system will be the foundation of this thesis. In order to control the UAVs in this flowfield, we proved that this system is controllable in Chapter 3. We proved that the deterministic nonlinear system formed by two vortices and with one then two tracers is controllable. This is the transition to Chapter 4 where the actual design of the control algorithm is developed now that we proved that such an algorithm can be implemented. Information rich location shall be taken in the sense of looking for the location in the space that, if the measurement is taken at that location, the entropy of the underlying random variable is reduced. The results were as expected where the conditional entropy is reduced when compared to the entropy of the vortex state without control. Furthermore, we encountered particular cases where the filtering algorithms without control diverge while the control brings back the data assimilation on the right path and the filtered signal tracks the real signal with minimal error.

One can use these results to improve current sensing systems. Indeed, the amount of data collected daily from observed systems is huge and getting out of control hence reducing the amount of information measured can be useful in this sense.

REFERENCES

[1] Agullo, O., Verga, A.: *Effect of viscosity in the dynamics of two point vortices: Exact results.* Phys. Rev. E 63(5):056304 (2001)

[2] Barreiro, A.K., S. Liu, N. S. Namachchivaya, P.W. Sauer and R. B. Sowers (2009) *Data Assimilation in the Detection of Vortices.* In: Applications of Nonlinear Dynamics Model and Design of Complex Systems, Springer, pp. 47-60. ISBN: 978-3-540-85631-3

[3] Chorin, A.J.: *Numerical study of slightly viscous flow. Journal of Fluid Mechanics* 57(4), 785–796 (1973)

[4] Ide, K., Kuznetsov, L., Jones, C.K.R.T.: *Lagrangian data assimilation for point vortex systems.* Journal of Turbulence 3:053 (2002)

[5] Jazwinski, A.H.: *Stochastic Processes and Filtering Theory.* Academic Press, New York (1970)

[6] Lugt Hans, J.: *Vortex flow in nature and technology.* Wiley (1983)

[7] Marchioro, C., Pulvirenti, M.: *Hydrodynamics in two dimensions and vortex theory.* Communications in Mathematical Physics **84**, 483–503 (1982)

[8] C. Marchioro, M. Pulvirenti, *Mathematical Theory of Incompressible Nonviscuous Fluids*, Applied Mathematical Sciences, Vol. 96, Springer-Verlag, 1994.

[9] P. K. Newton, *The N-Vortex Problem: Analytical Techniques*, Applied Mathematical Sciences Series, Vol. 145. Springer-Verlag, 2001.

[10] C. Paterson and D. A. Paley, *Multivehicle Coordination in an Estimated Time-Varying Flowfield*, Journal of Guidance, Control and Dynamics, Vol. 34, No. 1, January-February 2011.

[11] E. W. Justh, P. S. Krishnaprasad,*Equilibria and steering laws for planar formations*, 2003.

[12] R. Hermann, A. J. Krener, *Nonlinear Controllability and Observability*, IEEE Transactions on Automatic Control, Vol. AC-22, No. 5, October 1977.

[13] J.K. Hedrick, A. Girard, *Controllability and Observability of Nonlinear Systems*, Control of Nonlinear Dynamic Systems: Theory and Applications, 2005.

[14] A. Isidori, Nonlinear Control Systems: An Introduction, Springer Verlag, 1985.

[15] M. R. James, *Controllability and Observability of Nonlinear Systems*, University of Maryland, 1986, revised 1987.

[16] M. Ehrhardt, W. Kliemann, *Controllability of Linear Stochastic Systems*, Systems and Control Letters, Vol. 2, No. 3, October 1982.

[17] J. Zabczyk, *Controllability of Stochastic Linear Systems*, Systems and Control Letters, Vol. 1, No. 1, July 1981.

[18] Y. Sunahara, T. Kabeuchi, Y. Asada, S. Shin'ichi, K. Kishino, *On Sotchastic Controllability of Nonlinear Systems*, IEEE Transactions on Automatic Control, AC-19, p. 49-54, 1974.

[19] J. Klamka, E. Ferenstein, S*tochastic Controllability of Nonlinear Systems*, Proc ACMOS'11 Proceedings of the 13th WSEAS international conference on Automatic control, modelling & simulation, Pages 69-74, 2011.

[20] N. I. Mahmudov, S. Zorlu, *Controllability of non-linear stochastic systems*, Int. Joural of Control, Vol. 76, No. 2, p. 95-114, 2003.

[21] R. Sakthivel, J. -H. Kim, N. I. Mahmudov, *On Controllability of Nonlinear Stochastic Systems*, Reports on Mathematical Physics, Vol. 58, No. 3, 2006.

[22] G. Evensen, *Data assimilation, The Ensemble Kalman Filter*, 2nd ed., Springer, 2009 .

[23] A. H. Jazwinski, *Stochastic Processes and Filtering Theory.* Academic Press, New York, (1970).

[24] A. J. Krener, *Eulerian and Lagrangian observability of point vortex flow*, Tellus A, Vol. 60, Issue 5, p. 1089-1102, October 2008.

[25] R. E. Kalman, *A New Approach to Linear Filtering and Prediction Problems*, Transactions of the ASME–Journal of Basic Engineering, Vol. 82, Series D, p35-45, 1960.

[26] M.S. Arulampalam, S. Maskell, N. Gordon, T. Clapp: *A tutorial on particle filters for online nonlinear/non-Gaussian Bayesian tracking.* IEEE Transactions on Signal Processing **50(2)**, 174–188 (2002)

[27] Cover, Thomas M. and Thomas, Joy A., *Elements of Information Theory* (Wiley Series in Telecommunications and Signal Processing), 2006, Wiley-Interscience.